AFAPL-TR-77-10

(12)

DEMONSTRATION TESTING OF A VUILLEUMIER CRYOCOOLER WITH AN INTEGRAL HEAT PIPE/ THERMAL ENERGY STORAGE UNIT

ENERGY CONVERSION BRANCH
AEROSPACE POWER DIVISION

JUNE 1977

TECHNICAL REPORT AFAPL–TR–77–10
FINAL REPORT FOR PERIOD SEPTEMBER–DECEMBER 1976

D D C
RECEIVED
AUG 11 1977
A

Approved for public release; distribution unlimited

AIR FORCE AERO–PROPULSION LABORATORY
AIR FORCE WRIGHT AERONAUTICAL LABORATORIES
AIR FORCE SYSTEMS COMMAND
WRIGHT-PATTERSON AIR FORCE BASE, OHIO 45433

This report has been reviewed by the Information Office, (ASD/OIP) and is releasable to the National Technical Information Service (NTIS). At NTIS, it will be available to the general public, including foreign nations.

This technical report has been reviewed and is approved for publication.

JERRY E. BEAM/POE-2

TOM MAHEFKEY/POE-2

FOR THE COMMANDER

JOSEPH F. WISE
Technical Area Manager

REPORT DOCUMENTATION PAGE		READ INSTRUCTIONS BEFORE COMPLETING FORM
1. REPORT NUMBER AFAPL-TR-77-10	2. GOVT ACCESSION NO.	3. RECIPIENT'S CATALOG NUMBER
4. TITLE (and Subtitle) Demonstraction Testing of a Vuilleumier Cryocooler with an Integral Heat Pipe/Thermal Energy Storage Unit		5. TYPE OF REPORT & PERIOD COVERED Interim Test Report September-December 1976
		6. PERFORMING ORG. REPORT NUMBER N/A
7. AUTHOR(s) Jerry E. Beam Tom Mahefkey		8. CONTRACT OR GRANT NUMBER(s) N/A
9. PERFORMING ORGANIZATION NAME AND ADDRESS Aerospace Power Division/POE-2 Air Force Aero-Propulsion Laboratory Wright-Patterson AFB, OH 45433		10. PROGRAM ELEMENT, PROJECT, TASK AREA & WORK UNIT NUMBERS 21269310 31451949
11. CONTROLLING OFFICE NAME AND ADDRESS Aerospace Power Division/POE-2 Air Force Aero-Propulsion Laboratory Wright-Patterson AFB, OH 45433		12. REPORT DATE June 1977
		13. NUMBER OF PAGES 69
14. MONITORING AGENCY NAME & ADDRESS(if different from Controlling Office)		15. SECURITY CLASS. (of this report) UNCLASSIFIED
		15a. DECLASSIFICATION/DOWNGRADING SCHEDULE N/A
16. DISTRIBUTION STATEMENT (of this Report) Approved for public release, distribution unlimited		

17. DISTRIBUTION STATEMENT (of the abstract entered in Block 20, if different from Report)

18. SUPPLEMENTARY NOTES

19. KEY WORDS (Continue on reverse side if necessary and identify by block number)

Thermal Energy Storage
High Temperature Heat Pipe
Space Power
Vuilleumier Cryocooler

20. ABSTRACT (Continue on reverse side if necessary and identify by block number)

The performance of heat pipe/thermal energy storage unit (HP/TESU) powering a Vuilleumier (VM) cryocooler during simulated orbital eclipse periods was demonstrated. Operation with the HP/TESU was shown to have no significant cold stage performance penalty on the VM. The power consumption rate of the VM was determined to be approximately one-half the nominal design value (750 wt) due probably to high first stage heat leaks. VM cold stage performance was stable over large hot cylinder temperature variations (50-100°C). No thermomechanical or integration problems were incurred. Operation of HP/TESU as a combined thermal storage medium and hot cylinder heating mechanism is feasible.

DD FORM 1473 EDITION OF 1 NOV 65 IS OBSOLETE
1 JAN 73

FOREWORD

This in-house effort was conducted under Project 31451949 "Heat Transfer and Thermal Energy Storage Investigation," in support of the SAMSO sponsored Project 21260310 "Heat Pipe/Thermal Energy Storage Demonstration Unit".

The integral heat pipe/thermal energy storage unit (HP/TESU) was designed and fabricated under the direction of Dr. Robert Richter of Xerox/Electro Optical Systems, Inc.

This report describes the results of testing the Heat Pipe Thermal Energy Storage Unit with a Vuilleumier Cryocooler. The work was performed by the Aerospace Power Division's Energy Conversion Branch during the period September-December 1976. The technician support provided by Mr. Marvin Gaston, AFAPL/TF and Mr. Rick W. Nawman, AFFDL/FEE is acknowledged. The technical assistance provided by Mr. William Haskins, AFFDL/FEE and Dr. Dean Jacobson, Arizona State University, during the actual testing is acknowledged. The analysis of the data and conclusions are those only of the authors.

AFAPL-TR-77-10

TABLE OF CONTENTS

TABLE OF CONTENTS (Cont'd)

LIST OF ILLUSTRATIONS

LIST OF ILLUSTRATIONS (Cont'd)

LIST OF TABLES

SECTION I

INTRODUCTION

1. BACKGROUND

This report describes the results of initial performance verification and demonstration tests conducted on an integral heat pipe/thermal energy storage unit (HP/TESU) mated to a Vuilleumier cryocooler (VM). The HP/TESU was designed and fabricated by Xerox/Electro-Optical Systems, Inc., under contract AF33615-75-C-2045. Details of its configuration and performance are presented in the following paragraphs and more completely in Reference 1. The VM cryocooler was designed and fabricated by Hughes Aircraft Company (Reference 2). The VM control apparatus was modified by the Air Force Flight Dynamics Laboratory (AFFDL) to allow direct thermal, rather than electrical resistive, energy input to the hot cylinder. AFFDL also installed a modified vacuum dewar and cold stage resistive heaters and thermocouples.

The use of thermal energy storage, to provide heat energy to a VM cooler during orbital eclipse periods of surveillance spacecraft is motivated by the potential weight and reliability advantages of the HP/TESU concept over conventional and/or advanced electrochemical storage systems. Energy densities of 30-50 whr/lb are achievable with the HP/TESU concept, as contrasted to 4-10 whr/lb attainable with present and future secondary batteries, respectively, for low earth orbits.

2. PURPOSE AND SCOPE OF TESTING

The primary purpose of this testing effort was to demonstrate the inherent compatibility of the HP/TESU with a functional VM cryocooler. Under a company sponsored development program, Honeywell, Inc., demonstrated the operation of a VM cryocooler employing a heat piped hot cylinder under steady start-up and heat transfer conditions (Reference 3). Heat pipe "fired" Stirling engines, with hot cylinders similar to the VM hot cylinder, have also been demonstrated by Phillips (Reference 4). The specific objectives of this work were to demonstrate that the VM and

HP/TESU were compatible from a thermomechanical and integration standpoint, and that the transient, cyclic heat transfer processes occurring during the thermal charging and discharging of the HP/TESU imposed no significant performance penalty on the VM.

A secondary purpose of this testing effort was to evaluate VM performance under "off-design" conditions. The HP/TESU was designed to maintain the VM hot cylinder at 1250 $\pm$25°F (676.6 $\pm$13.9°C) at a 1 kw heat transfer rate, with a maximum storage capcity of 1 kw-hr. Tests were conducted at higher and lower hot cylinder temperatures and through larger thermal swings ($\Delta T = 100$°C). Tests at steady state heat transfer conditions were also conducted in order to estimate insulation heat losses and apparent, or effective, thermal conductivity of the HP/TESU. Additional tests to characterize the performance of the HP/TESU itself were conducted to evaluate the storage capacity anomaly reported in Reference 1.

To compare the performance of the electrically heated VM with that of the VM powered by the HP/TESU, a series of "baseline" electrically heated tests were performed in a fashion reported in References 2 and 3.

SECTION II

EXPERIMENTAL APPARATUS DESCRIBED

1. HUGHES "AFLIR" VUILLEUMIER CRYOCOOLER

The VM refrigerator employed is a liquid cooled, two-stage machine producing (nominally) 2 watts of cooling at 25°K and 3 watts at 75°K at ambient rejection temperatures of 300°K. The refrigerator system includes the cooler itself, a power inverter to drive the motor, a temperature/power controller, and an auxiliary coolant loop and heat exchanger. Figure 1 shows a schematic of the major components and instrumentation for the electrically heated configuration. Figure 2 is a photograph of the cooler with the conventional electrically heated hot cylinder installed.

The hot cylinder is approximately two inches in diameter and four inches long, with three separate heaters brazed to it. The heaters are Y-connected and operate on three phase, 200 vac line to line, 400 Hz power. Each heater provides a nominal 250 watts at 115 vac. Three sheathed, K-type thermocouples mechanically attached at the dome-shaped top of the hot cylinder, provide temperature and control signals in the electrically heated configuration. The hot cylinder and hot cylinder liner are of Inconel 718, with stainless steel (0.012 inch I.D., 0.022 inch O.D.) regenerator tubes tightly packed between the two surfaces.

In the electrically heated configuration, the temperature controller functions to maintain the hot cylinder at a nearly constant temperature of 1270°F +25°F (687.7°C +13.9°C), with a safety shut-off feature to prevent inadvertent overpressurization and overstress of the hot cylinder, should gas temperatures exceed 1400°F (790°C). The temperature controller operates one of the three hot cylinder heaters continuously and cycles the second or third one on and off, as required to maintain the hot cylinder in the 1270°F +25°F (688°C) control range. The temperature control set point can be manually adjusted to provide 1270°F +50°F regulation.

TEMPERATURE CONTROLLER

POWER INVERTER

BRAZED NICHROME HEATERS (3)

INSULATED HOT CYLINDER & REGENERATOR ASSEMBLY

CONTROL & REGULATING THERMOCOUPLES

COOLANOL 25 PUMP AND H/X

CRANKCASE

COLD STAGE THERMOCOUPLES &

RESISTANCE HEATERS
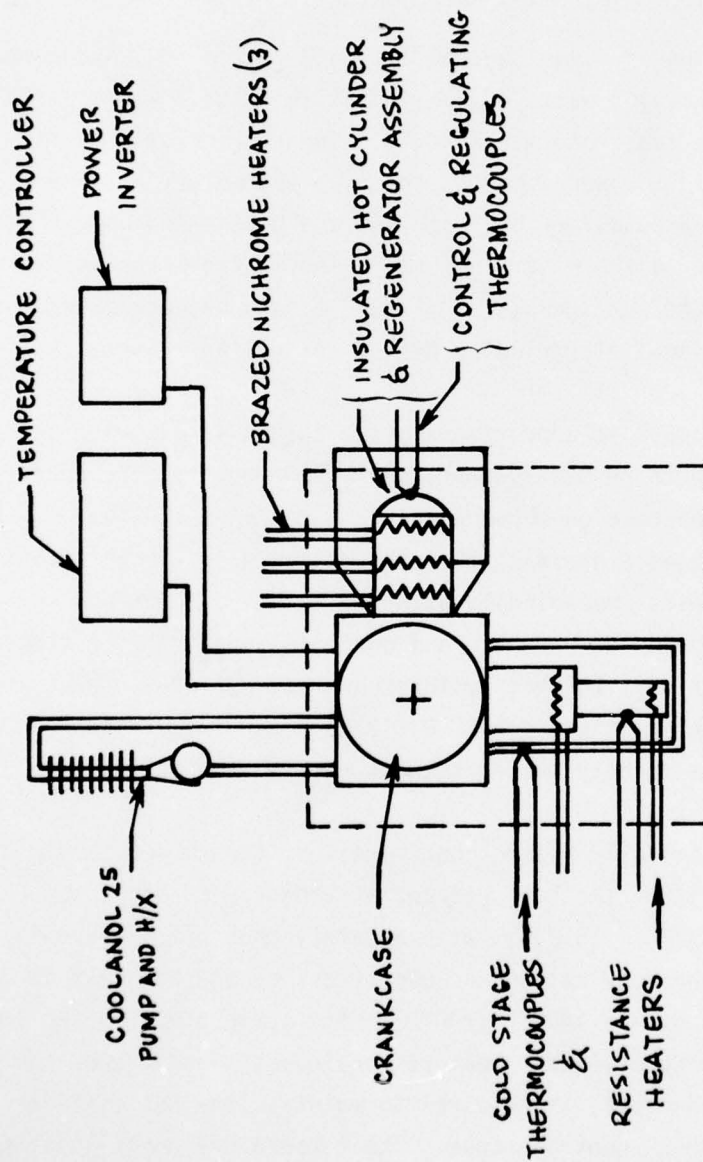
Figure 1. Electrically Heated VM Configuration Schematic

4

FIG. II-2.
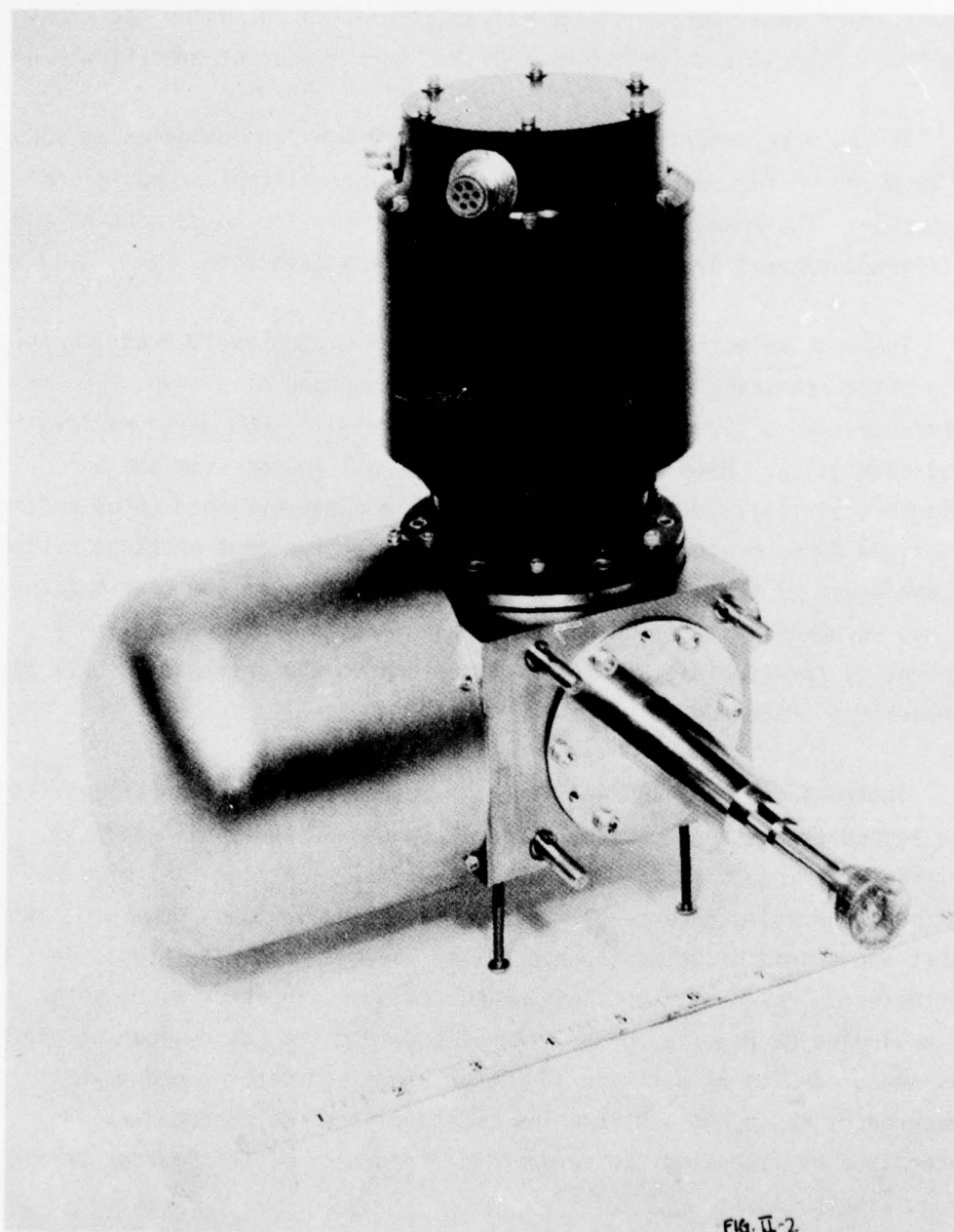
Figure 2.   Photograph of Electrically Heated "AFLIR" VM Cryocooler

The temperature controller was also equipped with manual control to permit short term operation with all three heaters on, which overrides the "two-heater-on, third-heater-cycling" normal mode of operation.

The power inverter transforms 400 Hz AC power for operation at 600 rpm or 28 DC power for operation at 900 rpm for intermittent or rapid cool-down operation. Two-speed adjustment potentiometers allow adjustment of the refrigerator speed by approximately +50 rpm for each mode.

The heat rejection unit circulates 1 gpm of Coolanol 25 at 120 psig to provide crankcase cooling. The unit is composed of a pump, a fluid reservoir, and a liquid-to-air heat exchanger with 1000 watts maximum load capability. With the exception of thermal losses from the hot cylinder, virtually all the input power to the hot cylinder (plus internal frictionally generated heat) must be removed by the heat exchange system. In the event of heat exchanger shut-down or failure of the heat exchanger, it was recommended that the helium working gas be vented immediately to prevent overpressurization of the system due to the increase in bulk gas temperature (Reference 5).

Instrumentation furnished with the system included crankcase, first and second stage thermocouples (Type T, Copper-Constantan), and hot cylinder thermocouples (K-type, Chromel-Alumel). Helium fill pressure was measured using an external Bourdon type gauge. Input power to the first and second stage resistance heater was measured with precision wattmeters. Power to first and second resistance heaters was generated by employing DC power supplies. Input power to the hot cylinder heaters was measured with AC wattmeters. Motor power and motor speed were measured by employing a strobe light tachometer. Motor speed was determined by assessing the fundamental frequency of the Bourdon pressure gauge fluctuations.

2.   XEROX/EOS HEAT PIPE/THERMAL ENERGY STORAGE UNIT

The HP/TESU employed was designed and manufactured expressly for
testing with the AFLIR cryocooler. The thermal energy storage (TES)
material, eutectic KF-LiF-MgF$_2$ (6-64-30 mole percent), which melts at
713°C (1315°F), is contained in a concentric annulus bounded by an inner
and outer sodium heat pipe. The inner and outer heat pipe share a common
condenser section, namely, the VM hot cylinder exterior wall and dome.
As shown schematically in Figure 3, the TES annulus also contains a
concentric heater well. The heater well contains Inconel sheathed,
ceramic insulated nichrome resistance heaters in a hairpin, U-shape
configuration.

The overall dimensions of the HP/TESU, neglecting the hot cylinder
regenerator zone, is approximately 18 inches in length and 10 inches in
diameter. The regenerator zone of the hot cylinder extends approximately
2 1/2 inches beyond the end of the heat pipe. The hot cylinder side
walls and dome extend into the heat pipe approximately 1 1/2 inches where
heat transfer with the heat pipe's sodium working fluid occurs. The
inner surfaces of the heat pipe, TES annulus, and hot cylinder walls and
dome are wicked by four to eight layers of 70 mesh Stainless Steel Bolting
Cloth which were spot welded to the Inconel 600 wall and Inconel 718 hot
cylinder, respectively. (Unfortunately, Inconel screen was not available
for use as a wick material.)

The end of the HP/TESU opposite the hot cylinder end contains the
heat pipe processing and fill valve; the thermal energy storage material
was loaded and sealed in the concentric annuli before loadint the heat
pipe.

Prior to delivery to AFAPL for testing with the VM the HP/TESU had
been tested with a gas flow calorimeter inserted in the VM hot cylinder.
Details of these tests and a complete description of the HP/TESU are
presented in Reference 1.

DRIVE MOTOR

COLD STAGE

HOT CYLINDER

THERMAL ENERGY
STORAGE SALT

ELECTRICAL HEATER

VAPOR FLOW PASSAGE

WALL WICK

OUTER SHELL

INSULATION
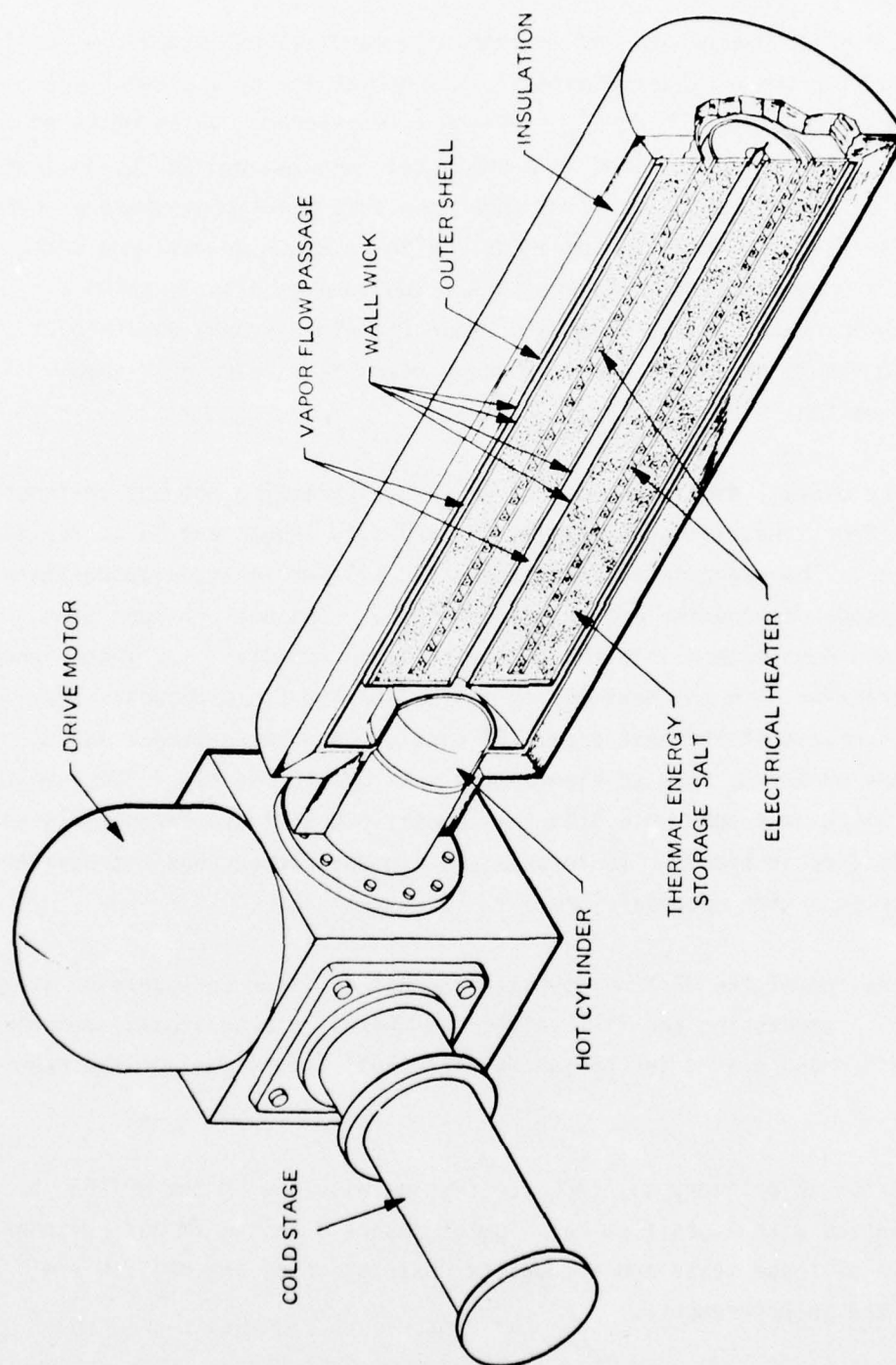
Figure 3. HP/TESU-VM Configuration Drawing

Figure 4 presents a schematic of the integrated HP/TESU-VM units and related auxiliary and instrumentation apparatus. This configuration is nearly identical to that shown in Figure 1 with the following exceptions: the electrically heated hot cylinder has been removed from the VM and replaced by the integral HP/TESU; the temperature controller function was bypassed and a manually controlled 220V variac power supply substituted to power (thermally charge) the HP/TESU, thus supplying heat to the VM cryocooler. A precision wattmeter was employed to measure input electrical power during the charging of the HP/TESU. Discharge of the HP/TESU was accomplished manually by turning off the electrical power to the HP/TESU's heaters while the VM continues to operate on the energy stored in phase change TES salt and the sensible heat of the HP/TESU. At the end of a thermal discharge the HP/TESU heaters are again energized and the VM continues to operate without interruption while a fraction of the input power recharges (remelts) the TES material. Figure 5 shows the actual test setup and hardware.

Operation of the system is partially analogous to electrical energy storage in an electrochemical battery. The HP/TESU concept differs in the sense that the thermal storage material and thermal load (VM cryocooler) are in thermal series during both the charging and discharging operations as contrasted to the electrochemical battery-VM system, where the battery and VM are electrically parallel loads during charging. Both would employ a solar cell array to provide power to the VM during sunlit portions of the spacecraft orbit.

3. INSTRUMENTATION ACCURACY

The instrumentation provided by AFAPL included thermocouples, pressure gauge, and wattmeters, and motor speed tachometer. The temperature and electrical power input measurements were considered to be the most significant. To measure temperature, two procedures were employed. For temperatures within the limit of -200°C to 1000°C, a multipoint digital voltmeter was employed. This instrument converts thermocouple voltage with conformance error of ±0.5°C over this range and was calibrated

9
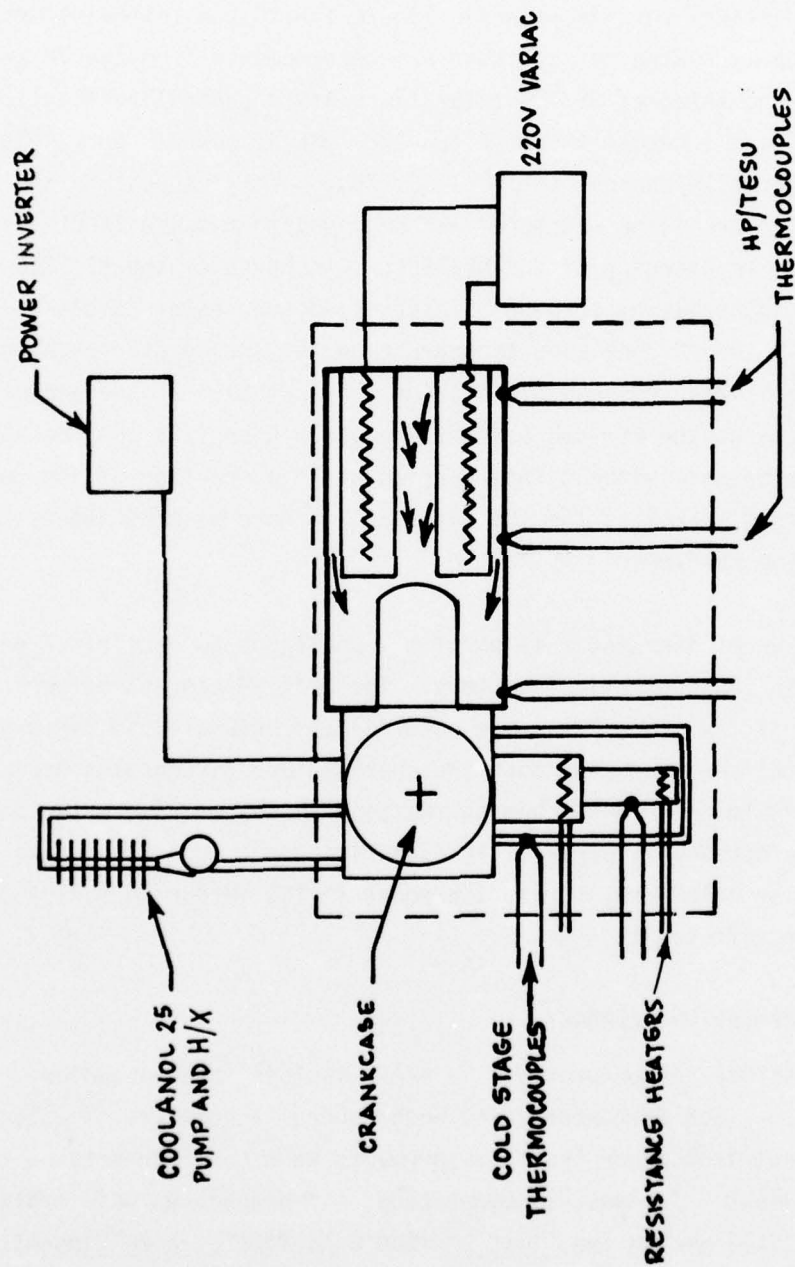
Figure 4. Integrated HP/TESU-VM Configuration

10
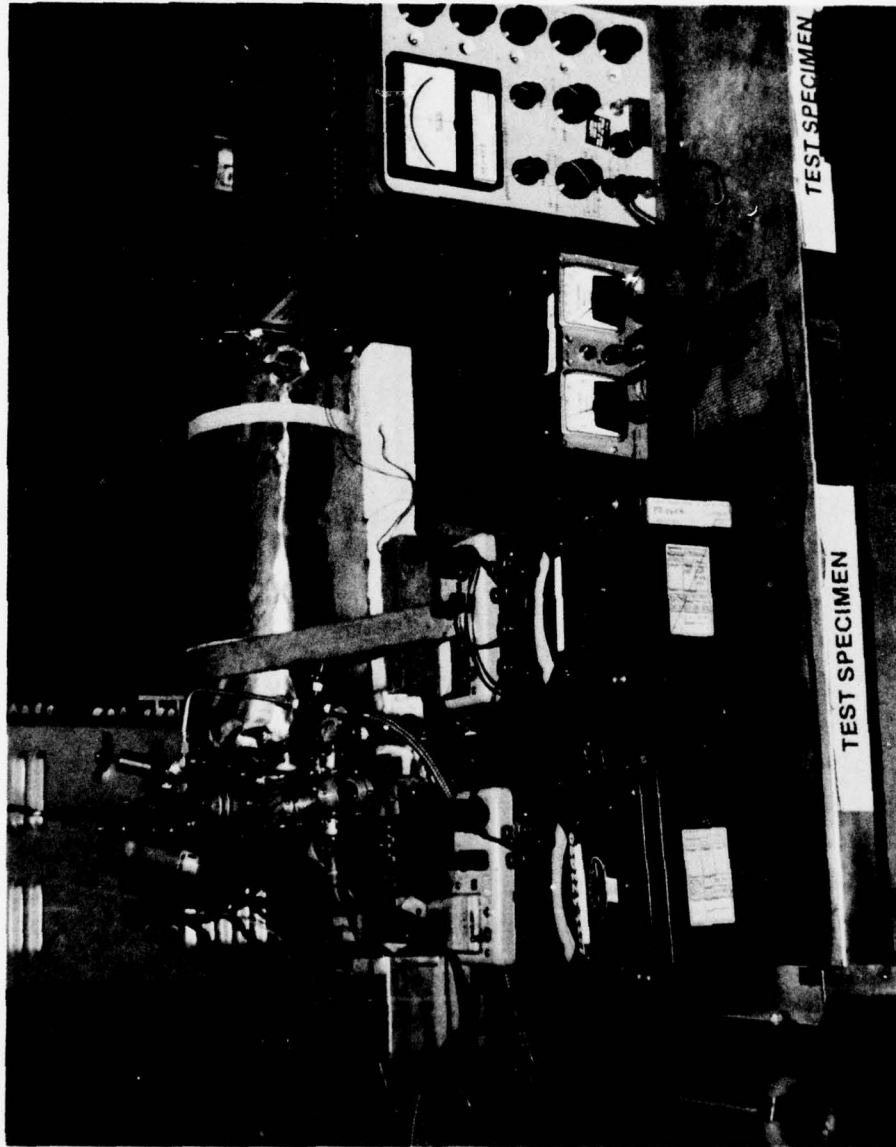
Figure 5. Photograph of Integrated Test Hardware

by the manufacturer using standards whose accuracies are traceable to the National Bureau of Standards. Thermocouples used with this instrument were of the ANSI standard grade Type-K, chromel-alumel. Only calibrated thermocouples were employed and the standard limits of error were given as $\pm 2.5°C$ from 0 to 275°C and $\pm 3/4\%$ from 275 to 1250°C. To minimize temperature measurement error in the heater well the sheathed thermocouples were fitted with tubular stainless steel radiation shields, so that only the tip of the thermocouple was exposed, thereby localizing the temperature measure. For temperature measurements below -200°C, an electronic reference junction and a 0.01 mv resolution AC/DC differential voltmeter were employed to measure the thermocouple voltage. The reference junction provides a constant voltage simulating 77°K reference temperature. The junction was calibrated by zeroing the junction's output voltage while measuring the temperature of boiling liquid nitrogen at one atmosphere. This calibration was then checked using boiling distilled water at one atmosphere and proved to have less than 0.1% error. As a second check, the data obtained using the digital thermometer was compared with that obtained using the reference junction. These results compared within 1°C of each other.

To measure the electrical power input, "precision" electrodynamometer wattmeters were used. The manufacturer's published accuracy of this meter type is given as 1/4 of 1% of full-scale deflection. To evaluate this accuracy, several no-load tests were conducted, the results of which easily fell within these limits. Under load conditions, an additional voltmeter and induction ammeter were connected to verify the wattmeter reading. These tests also indicated agreement with the wattmeter reading. Several sample meter correction calculations were made during the course of the testing but all calculations indicated insignificant error being introduced by the wattmeter. As a general evaluation of accuracy, all wattmeter readings are estimated within $\pm 3\%$ of the actual value.

4.   HP/TESU-VM INTEGRATION

The HP/TESU, as received from Xerox EOS, needed only the addition of a hot cylinder piston liner and the tubular regenerator elements. These parts were removed from a spare VM (SN #1) cooler and installed in the HP/TESU prior to the integration of HP/TESU and VM (SN #2).

The regenerator elements removed from the spare VM were heavily coated with a carbonlike deposit and it was conjectured that the tubes may be partly restricted. Prior to installation, the regenerator tubes were cleaned with aircraft engine carbon solvent and degreaser, methol alcohol, acetone, and DI water. As a final check, a random sample of approximately 1/3 of the regenerator tubes was checked for blockage with a 10 mil wire. No indication of a blocked or restricted passage was observed. The cylinder liner and regenerator system were then pressed into HP/TESU.

The sole means of mechanically attaching and sealing the HP/TESU to the VM was a split flange. The nonavailability of Inconel stock of the desired size limited this configuration to a split (non-integral) flange design. This split flange required an additional high pressure seal to effect a seal between the HP/TESU and the VM. The seal design selected was a 1/32 inch x 2 3/8 inch I.D. silver plated Inconel metal O-ring sealing groove. A 1/32 inch thick backup plate was fabricated such that the O-ring could not deform radially away from the sealing edge. The first O-ring supplied by Xerox was 2.438 inch O.D. x 1/32 inch thick with a 20 mil thick backup plate. This seal would not hold. It was assumed that the problem evolved from not being able to center the ring on the sealing surface. A thicker O-ring was then obtained. A 2.445 inch O.D. x 1/16 inch O-ring and a 40 mil thick backup ring were used in the second attempt. This new O-ring fit quite tightly around the TESU and no slippage was possible. While using the split flange as a guide to fabricate a new backup ring, it was discovered that the flange was warped. Warping was surmised to have occurred due to stress buildup during the machining, with subsequent warpage when the flange was split.

After re-working the flange, the thicker 1/16 inch O-rings and 40 mil backup ring were installed, and the seal effected. The 20 mil O-ring supplied by Xerox/EOS would probably have worked equally well if the split flange had not warped.

The only difference in the mechanical interface between the HP/TES-VM unit and the electrically heated VM unit is the addition of the backup and O-rings. These rings, in effect, increased the volume of the working gas by the area of the displacer and the thickness of the backup ring. This resulted in a slightly larger volume of gas in the hot cylinder during compression. It was found this small volume increase, less than 1/4 in^3, had no apparent effect on the VM performance.

SECTION III

EXPERIMENTAL APPROACH AND RESULTS

1. APPROACH

Three types of tests were conducted during this initial test program. The objectives and approaches of each phase are summarized in the following paragraphs.

2. VM PERFORMANCE CHARACTERIZATION

To establish a comparative baseline of cooler performance in the as-received condition, the VM was subjected to a limited series of tests using the manufacturer's electrically heated hot cylinder. These tests were not comprehensive nor thorough for two reasons: first, the VM cooler, as received at AFAPL, had already been subjected to over 1000 hours of testing since the last major overhaul, and the number of spare parts available for cooler repair in the event of a breakdown was extremely limited; second, the major purpose of the test program was to evaluate VM cooler performance with the HP/TESU. Electrically heated performance data under load and no-load conditions had already been performed by Hughes in the development of the cooler, and more recently by Honeywell (References 2, 3). Honeywell's investigation showed that the VM can be operated at constant power and/or constant temperature, albeit within certain limits (Reference 3).

The nominal demonstrated performance of the AFLIR VM is summarized in Table I for no-load and load conditions. Off-design performance data for several fill pressures, motor speeds, hot cylinder temperatures, and input powers are presented in Reference 1.

Table II summarizes the results of electrically heated baseline tests performed at AFAPL; the mean minimum first and second stage temperatures differ significantly from those reported in References 2 and 3. It appears that the performance of the VM may have degraded and/or the modifications performed at AFFDL (installing the first and second stage

15

TABLE I

DEMONSTRATED "AFLIR" VM PERFORMANCE (REFERENCE 2)
WITH ELECTRICALLY HEATED HOT CYLINDER

Refrigeration Load	No Load	Simultaneous 3W/2W 1st and 2nd Stage Loads
Minimum 1st Stage Temperature	40°K/-233°C	62°K/-211°C
Minimum 2nd Stage Temperature	17°K/-256°C	30°K/-243°C
Hot Cylinder Temperature	687.7°C (1275°F)	687.7°C (1275°F)
Crankcase/Heat Rejection Temperature	44.4°C/21°C	44.4°C/21°C
Motor Speed	600 rpm	600 rpm
Heater/Total Power Input	600 W_t/1015 W_e^* (*estimated)	730 W_t/1245 W_e
Insulation Losses	120 W_t	120 W_t
Helium Fill Pressure	675 psia	675 psia

TABLE II

BASELINE AS-RECEIVED VM PERFORMANCE
WITH ELECTRICALLY HEATED HOT CYLINDER

Fill Pressure	Hot Cylinder Temperature	Stage Loads 1st/2nd	1st Stage Temperature	2nd Stage Temperature	Crankcase Temperature
677 psia	650 +7°C	0/0W	-163°C	-221°C	32°C
675 psia	690 +7°C	0/0W	-169°C	-250°C	32.5°C
680 psia	680 +7°C	0/0W	-141°C	-242°C	41.9°C
675 psia	680 +7°C	0/0W	-153°C	-250°C	42.8°C
675 psia	690 +5°C	0/0W	-154°C	---	44.8°C
675 psia	680 +5°C	3/2W	-50.8°C	-202°C	41.2°C
672 psia	645 +5°C	3/2W	-42°C	-199°C	34.6°C
675 psia	685 +5°C	3/2W	-53°C	-226°C	33°C
680 psia	640 +10°C	3/2W	-46.7°C	-199.1	35°C
670 psia	685 +5°C	3/2W	-51°C	---	42°C

heaters, thermocouples, and a modified vacuum dewar) have increased the
heat load on the cold stages, as compared with the device tested by Hughes
and Honeywell (Reference 5).

The scatter in data is due in part to the variation in the crankcase
temperature and helium fill pressure from test to test. During this
phase the power inverter failed and was replaced, resulting in a noticeable
difference in hot cylinder regulated temperature.

To more fully characterize VM performance, additional tests with the
electrically heated VM were conducted, measuring both the motor speed and
heater power consumption. In the design speed range of 500-600 rpm the
heat input to the hot cylinder was approximately 500 watts under no-load
conditions, and 600 watts for the 3w/2w first and second stage load
conditions. Some scatter in this data was also observed; cold stage
temperatures were similar to those reported in Table V.

Figure 6 illustrates a typical transient no-load cool-down and
cooler thermal response to stage loading. The cool-down and transient
load response are comparable to previously reported data. As shown in
Figure 7, the hot cylinder cool-down and cold stage heat-up, when the
heater power is switched off, is rapid, and proportional to the low
thermal mass of this configuration.

3.   HP/TESU EQUILIBRIUM TESTS

The thermal insulation losses from the HP/TESU were measured in a
series of steady state heat transfer tests. The tests were conducted by
insulating the heat pipe fill tube and regenerator section of the hot
cylinder. Similar tests were conducted by Xerox/EOS during the checkout
of the unit, but it was thought advisable to remeasure the losses, since
the insulation on the unit had been modified for shipping and the shipping
of the unit might have compressed or damaged the insulation, hence
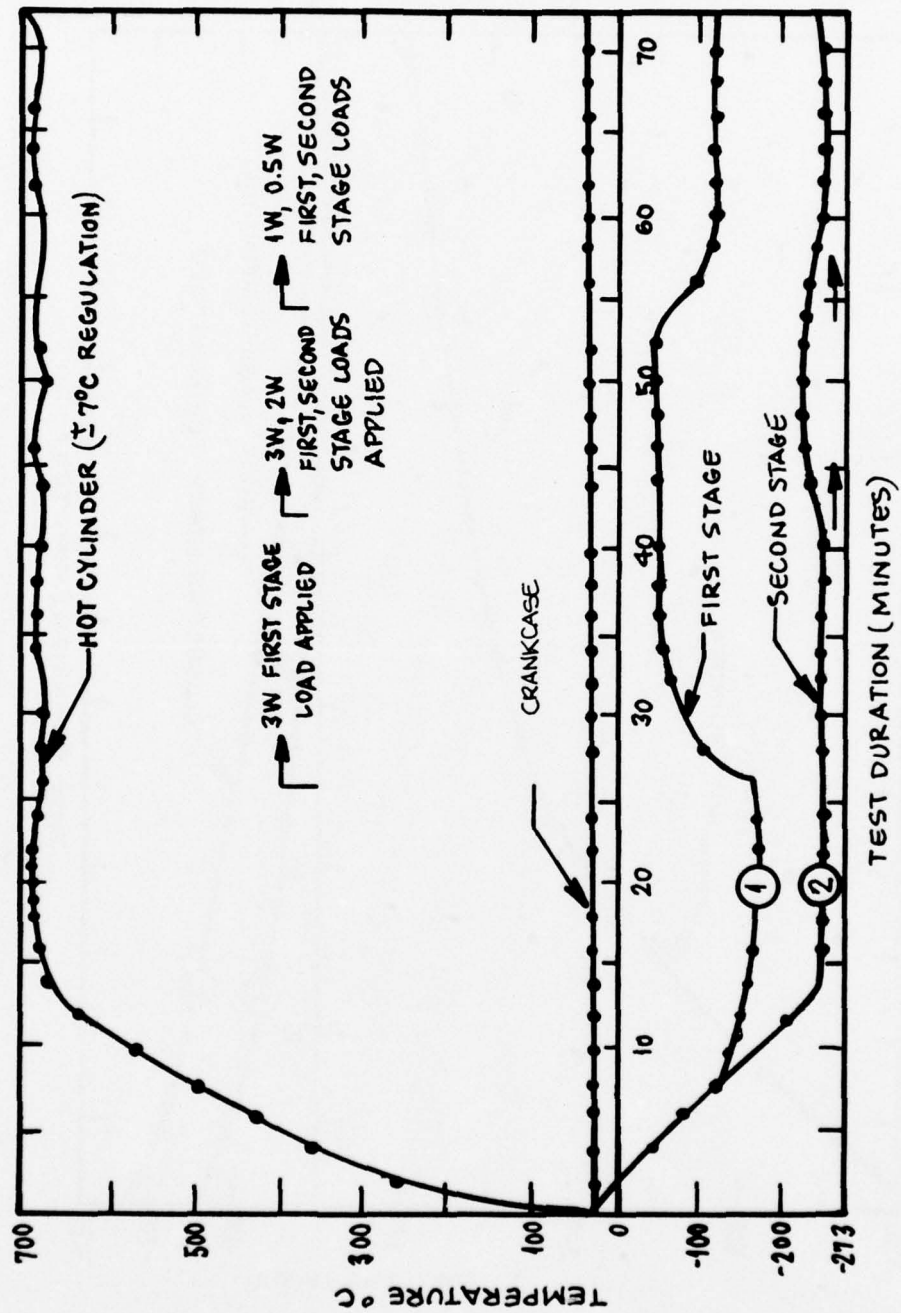increased the losses.

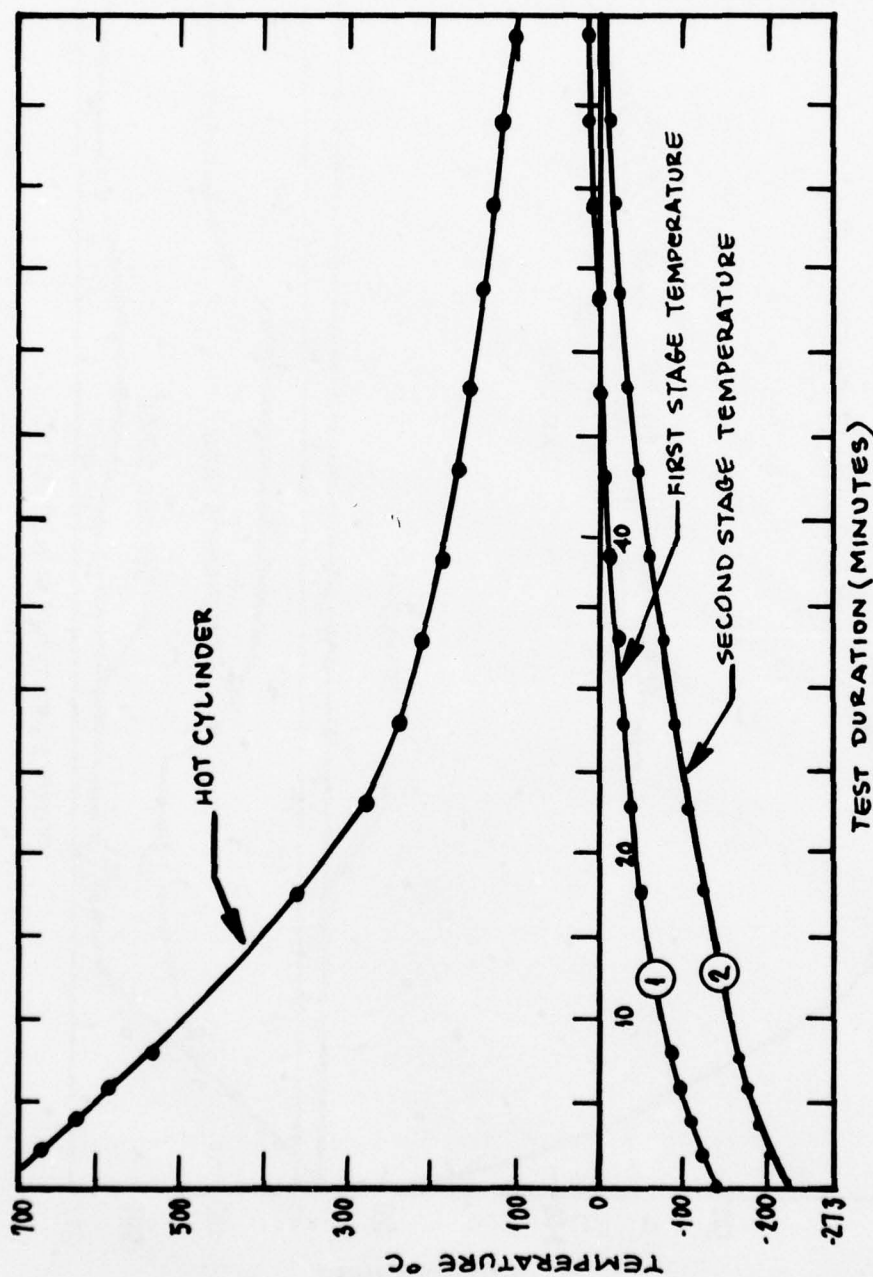Figure 6. Typical Electrically Heated VM Transient Performance, Start-Up

19

Figure 7. Typical Electrically Heated VM Performance During Heater Off
Operation, Cold Stages Unloaded

20

Figure 8 compares the insulation losses as measured at AFAPL and Xerox. Agreement is good. It should be pointed out that the equilibrium time for these measurements is extremely long (on the order of 10-100 hours) and that absolute equilibrium was difficult to obtain due to daily temperature variations in the laboratory ($\pm5°C$) and line-voltage variations (hence power variation) to the heaters.

Several radiatively cooled equilibrium tests were also conducted on the HP/TESU prior to integration with the VM. For these tests the insulation was removed from the hot cylinder regenerator section of the HP/TESU (prior to installation of the regenerator tubes and liner). Figure 9 shows the temperature profile for several of the higher temperature, fully insulated, and radiatively cooled hot cylinder tests. Note that the temperature profiles for the 150W fully insulated test are approximately the same as that obtained for the 240W radiatively cooled test. Similarly, the temperature profiles for the 200W fully insulated test and the 300W radiatively cooled test are nearly identical. Although no quantitative conclusions can be drawn from the data presented in Figure 9, a qualitative analysis shows that the equilibrium temperature of the heat pipe is a function of external resistance to heat transfer, as expected from basic heat transfer theory. Figure 10 shows similar data for three steady state external heat transfer conditions, namely, radiative cooling at an applied power of 340 watts, and those temperature profiles obtained after integration with the VM. Two cases are shown for the VM-installed configuration, one with the VM operating (motor on) and one with the VM pressurized but not operating as a refrigerator (motor and heat exchanger off). These data also illustrate qualitatively the equilibrium temperature, an external resistance heat transfer relationship. Since the temperature profiles for the VM "on" and VM "off" cases are so similar (including the regenerator section characterized by thermocouples 10, 11, and 12, it may be concluded that the net approximate heat transfer to the VM is approximately 400 watts (600 - 200W losses). Further analyses and additional data on the equilibrium tests will be described in Section IV.
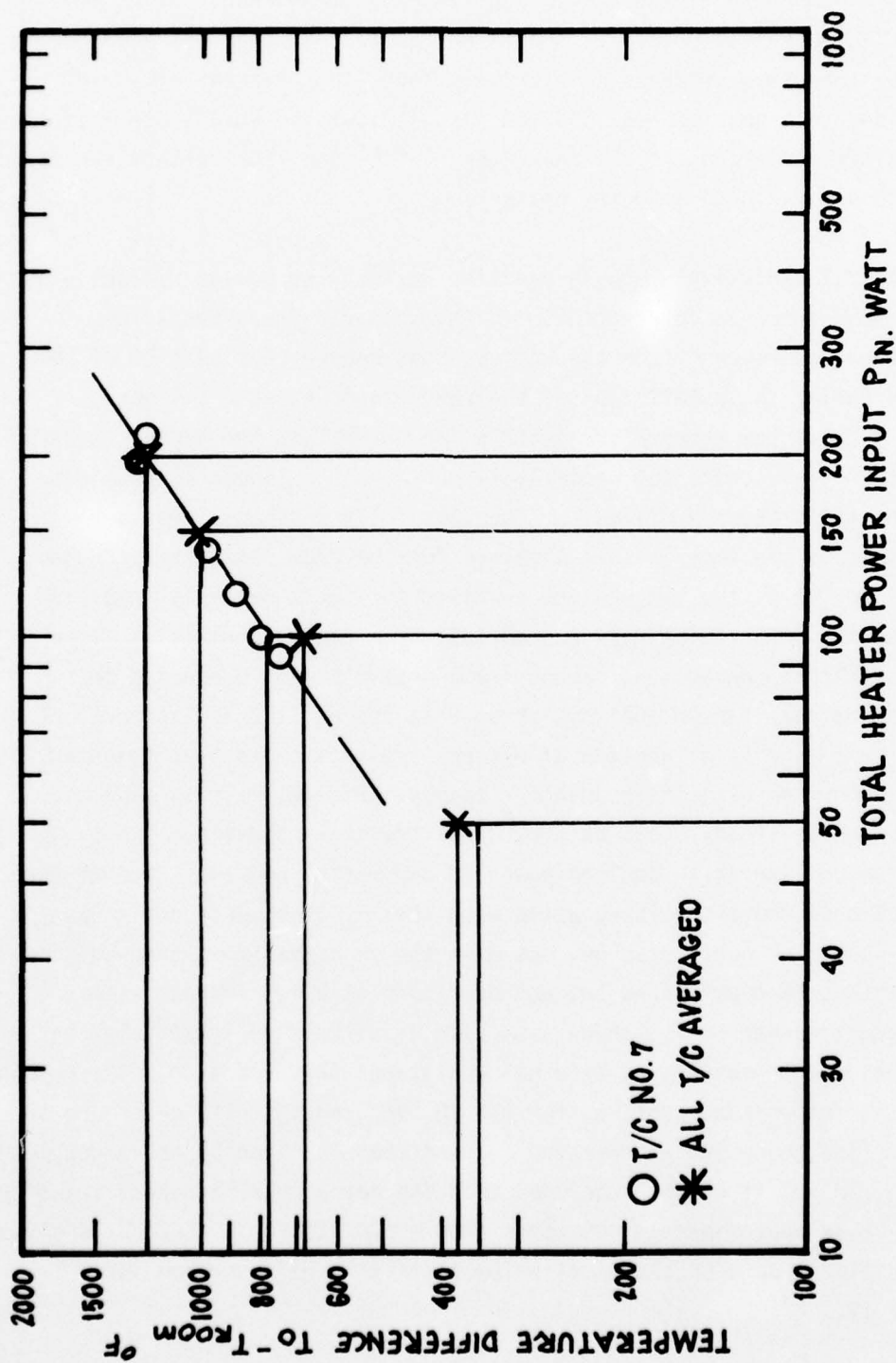
Figure 8. Heat Losses from HP/TESU
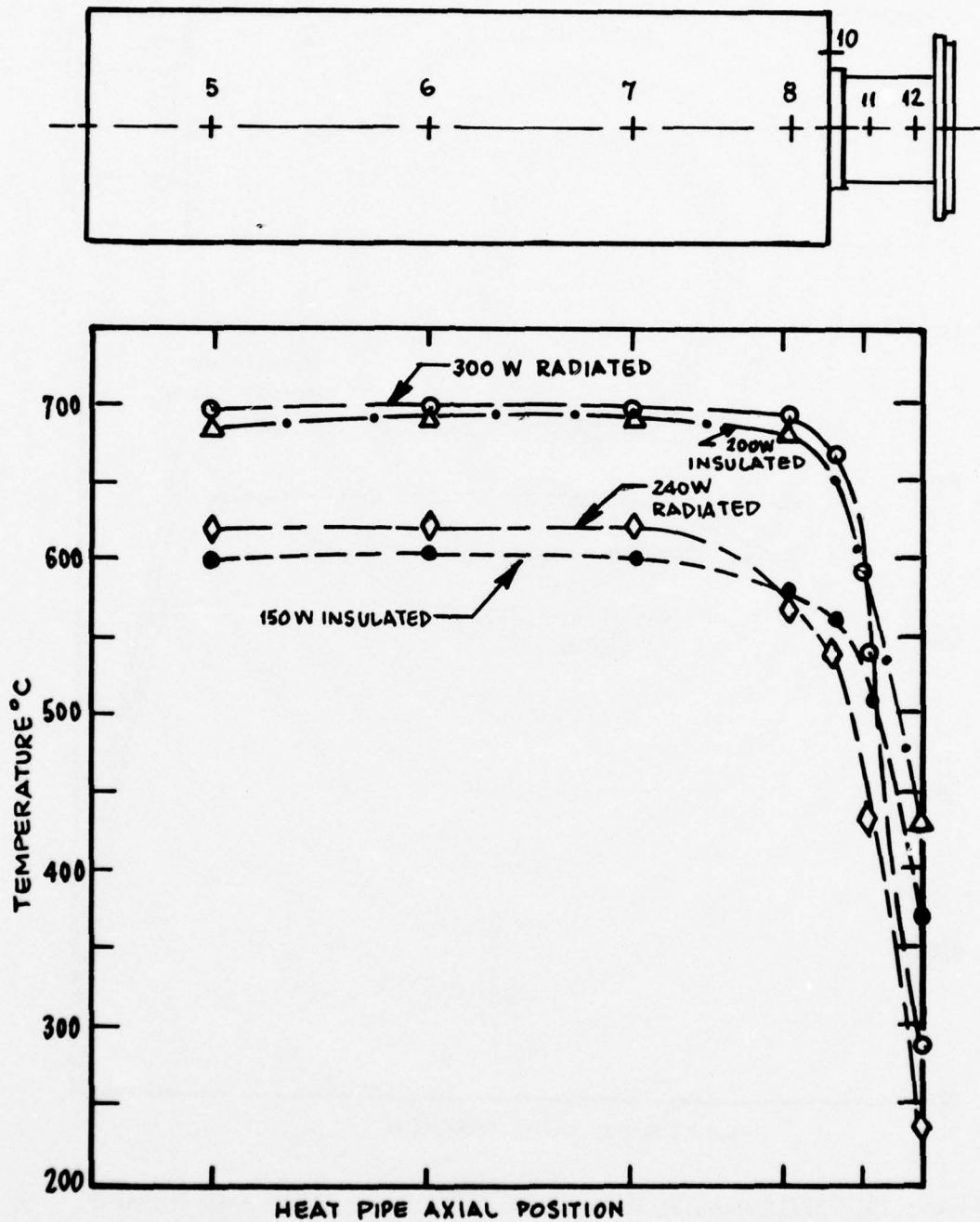
Figure 9.   HP/TESU Axial Temperature Profiles for Fully Insulated and
Radiatively Cooled Hot Cylinder
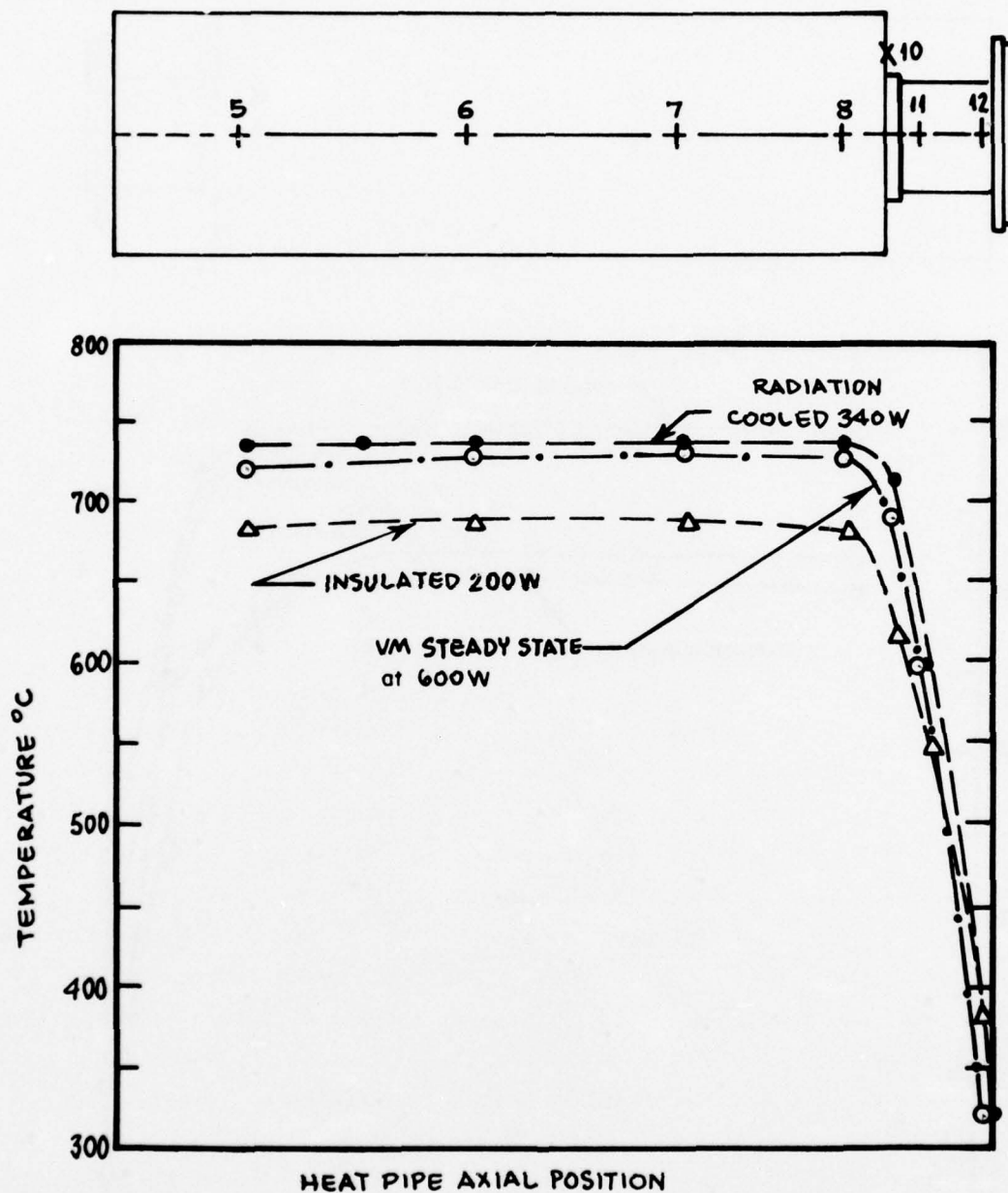
Figure 10. HP/TESU Axial Temperature Profile for Three Heat Transfer Conditions

4.   HP/TESU-VM START UP, STEADY STATE, AND CYCLIC MODES

Three categories of tests were performed on the integrated HP/TESU-VM system. The transient start-up characteristics from ambient and elevated (500°C) temperature at several heat input rates were measured. Steady state operation of the HP/TESU-VM was also evaluated. Cyclic performance of the HP/TESU-VM system between several hot cylinder (heat pipe condenser) temperature extremes corresponding to several charge/discharge time periods, were evaluated. Test results for each category of test are reported below.

a.   Transient Start-Up Characteristics

Figure 11 shows the time-temperature response for a HP/TESU-VM start-up from ambient (25°C) temperature. In this test, the system was initially at room temperature, with the VM charged to 675 psia. Simultaneously, the HP/TESU heaters were turned on to a setting of 1000 watts, and the VM inverter turned on to power the motor-displacer assembly. Figure 11 shows that the shielded thermocouples at end and mid-heater well positions heat at virtually the same rate, while the shielded thermocouples contacting the heater well end wall at the VM or condenser end of the HP/TESU lag significantly. The thermocouples located axially on the external surfaces of the (outer) heat pipe wall of the HP/TESU exhibit a normal axial evaporator to condenser temperature gradient; the time-temperature response of the thermocouples located near the VM end of the HP/TESU (i.e., condenser zone of the heat pipe) lag those thermocouples located at the fill tube and mid-section of the HP/TESU (evaporator zone). As test time approaches 240 minutes, the thermal arrest of mid-heater well thermocouples (E,F,M) at or near the eutectic temperature (713°C) is evident, indicating that melting of the salt was underway. The heater well thermocouples at the VM end (T,B) continue to lag significantly. Unfortunately, the test was interrupted at 250 minutes due to an open circuit failure of the heater. It is concluded that the start-up was nearly complete but the system had not reached equilibrium.

TEST DURATION (MINUTES)
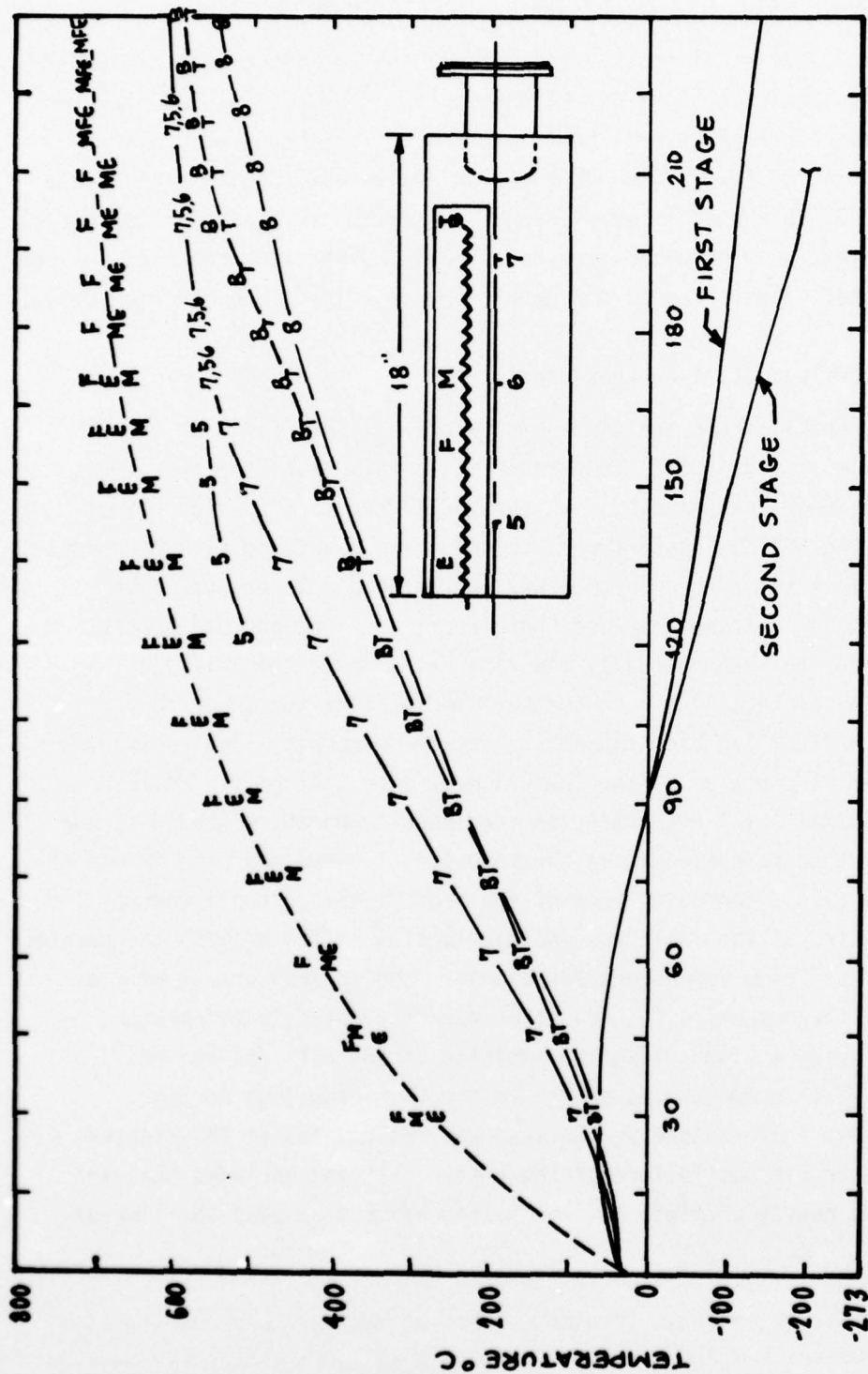
Figure 11. HP/TESU-VM Start-Up Transient Performance, 1000 Watts Applied

The VM performance during the 1000 watt start-up test is also shown in Figure 11. The first and second stage temperatures track each other through the first 90 minutes of test and then diverge in a manner similar to that observed during the electrically heated hot cylinder tests. The minimum first stage temperature achieved during this start-up test was -141°C. Second stage temperatures below -200°C were not measured due to test operator error.

b. HP/TESU-VM Steady State Tests

Figure 12 shows similar start-up data for a constant heating rate of 1200 watts. The test was conducted after the heater failure cited above was remedied and the heater well thermocouples reinstalled. The 1200 watt charge rate was selected based on an anticipated VM thermal input power of approximately 750 watts and thermal insulation losses of approximately 200 watts. Thus, approximately 250 watts (1200W - 950W) of electrical power would be available to increase the stored thermal energy of the HP/TESU. The test was conducted in the same fashion as described for the 1000 watt start-up test, with the exception that the HP/TESU was preheated to approximately 200°C (as measured by the external HP/TESU thermocouples) by applying 600 watts for 2 hours with the VM motor off to shorten the transient time. The data shown in Figure 12 shows a relatively rapid start-up. The front (fill tube end) and mid-heater well temperature exhibit a thermal arrest at approximately 120 minutes through 230 minutes, changing only by 20°C during that period (from 730°C to 750°C). As in the 1000 watt start-up test, the VM end heater well temperature and the heat pipe condenser thermocouples track each other closely during the entire test and lag the front and mid-heater well temperatures significantly over the first three hours of the test.

In an attempt to establish equilibrium and prevent overheating of the hot cylinder, the applied power was reduced to 1160 watts at 216 minutes. Further reductions of power were made (1140 watts at 232 minutes, 1100 watts at 255 minutes, 1020 watts at 278 minutes, and 1000 watts at 285 minutes). The temperature of the heat pipe and the heater well approached 800°C and 755°C respectively, at this time. The

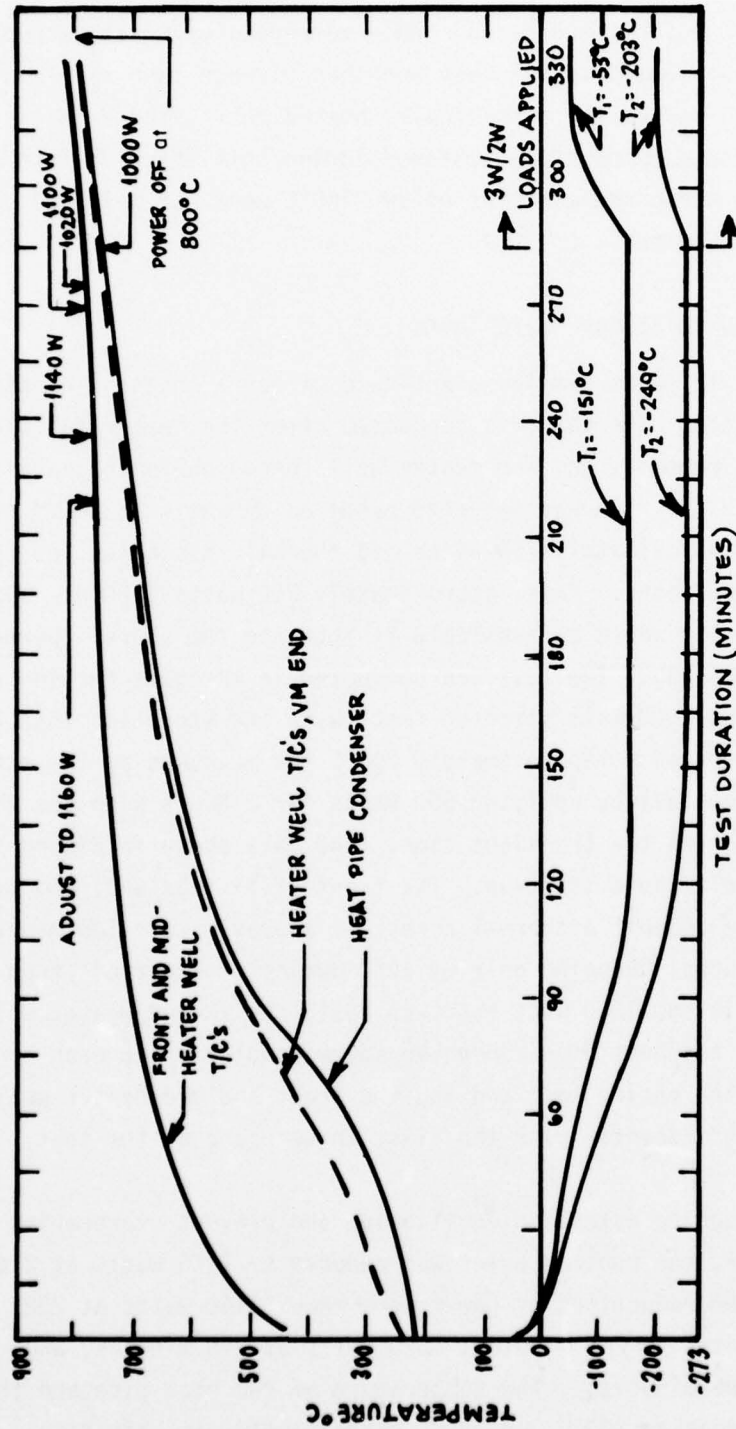Figure 12. HP/TESU-VM Start-Up Transient Performance, 1200 Watts Applied, No-Load and 3W/2W First/Second Stage Loads

first and second stage resistive loads were then applied. The temperature
of the cold stages immediately decreased, but the temperature of the
HP/TESU continued to increase. When the heat pipe condenser section
reached 800°C (100°C above the maximum) hot cylinder design temperature,
the power was turned off and the test terminated. The VM performance
was essentially constant after the thermal arrest was achieved and was
equivalent to that observed in the electrically heated baseline tests.
It was concluded that the VM power consumption plus thermal losses were
much less than 1000 watts (even at temperatures 100°C above the design
temperature).

A third attempt to obtain dynamic equilibrium (VM operating) after
start up is depicted by Figure 13. The HP/TESU was preheated to 500°C
to shorten the equilibrium time. The VM motor and heat exchanger were
turned on and 600 watts were applied to the HP/TESU heater. As noted in
the other start-up tests, the heat pipe condenser and VM end heater well
thermocouples tracked each other nearly identically and lagged mid and
end heater well temperatures by approximately 80°C during most of the
test. After 240 minutes the heat pipe temperature was essentially
isothermal (~5°C end to end variation). The test was intentionally
terminated when the heat pipe condenser temperature reached 600°C.
Peculiarly, the cold stage performance was nearly identical to that
achieved in the previous test with the heat pipe condenser temperature
at 750°C; first stage temperatures were -151°C (600°C) vs -158°C (750°C)
and second stage temperatures were -240°C (600°C) vs -249°C (750°C). As
can be seen in Figure 13, the temperature of the heat pipe was increasing
slightly when the test was terminated (~10°C/hour). Equilibrium was not
obtained (after 7 1/2 hours of constant 600 watt heat input with the VM
operational. During this period the HP/TESU temperature increase was
only 100°C. Since the thermal insulation losses at a heat pipe equilibrium
temperature of 600°C were measured to be 150 watts, the VM power con-
sumption had to be less than 450 watts (600 watt minus 150 watt losses
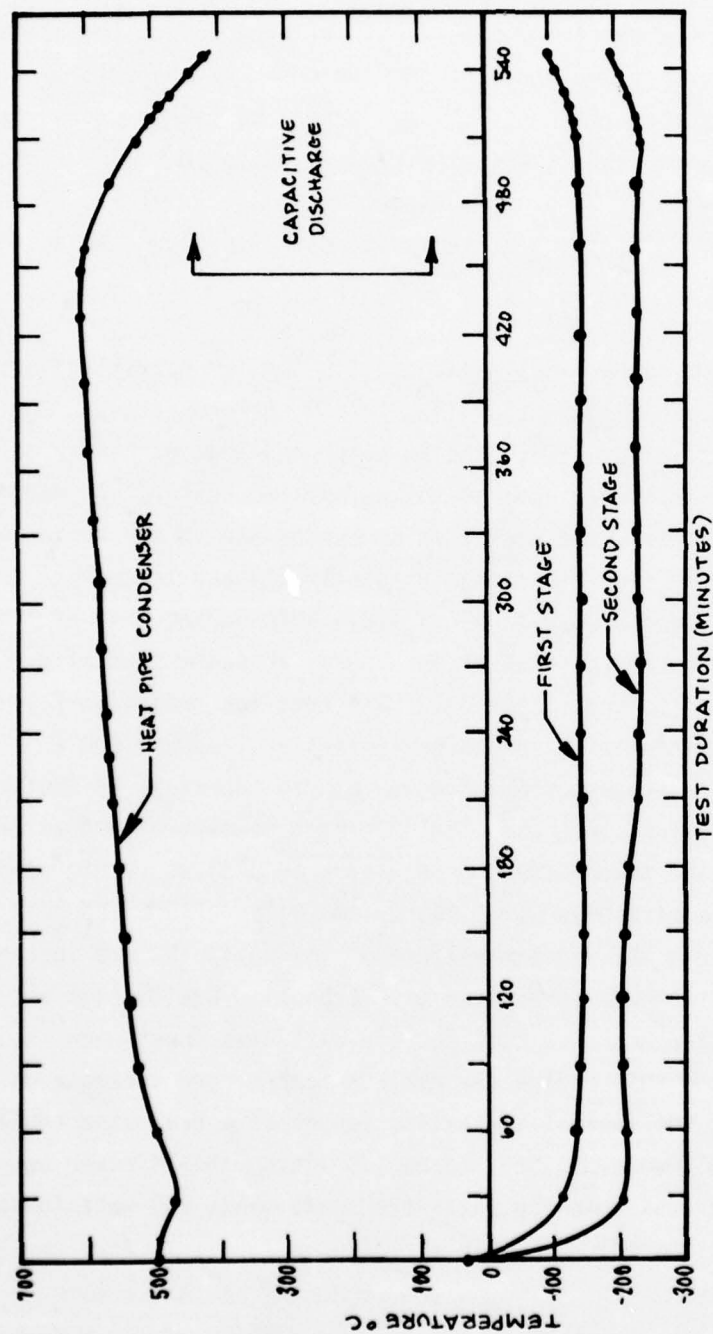minus rate of heat stored).

Figure 13. HP/TESU-VM Start-Up Transient Performance, 600W Applied, No-Load on Cold Stages

The fourth attempt to obtain dynamic equilibrium (VM operating) after start-up was successful. The test data are shown in Figure 14. The HP/TESU was preheated to 500°C with the VM not operating. A constant heat rate of 900 watts was applied for 5 1/2 hours. Power was cut back to 840 watts when the heat pipe temperature exceeded 700°C and the heater well temperature attained 750°C. The power was turned off temporarily at 354 minutes for a 20-minute period to cool the system. After the power was again turned on at a reduced level, the temperature continued to increase, although the power was continuously decreased in 40 watt increments at 15 minute intervals. Finally, the power was reduced to 600 watts and both the heater well temperature and heat pipe temperature stabilized at 749°C and 720°C, respectively, during a period of time from 430 minutes to 490 minutes. At 498 minutes, the cold stage loads were applied and the temperature of the heat pipe remained constant (720°C) through the next 20 minutes and decreased only 3°C after one hour with the cold stages loaded. The loaded (3W/2w cold stages reached -51°C and -203°C, respectively.

c. Thermal Cycling Tests

To evaluate the performance of the HP/TESU-VM system in the thermal charge, and the thermal discharge mode, a series of constant heat rate (1200 watt) tests were performed. Discharge tests were performed for periods up to 3 hours. During the tests, the HP/TESU and VM cold stage temperatures were monitored simultaneously. These test results are described in the following paragraphs.

d. Low Temperature Cyclic Test

Figure 15 shows the HP/TESU and VM cold stage temperatures for consecutive 1200 watt heating half cycles to 600°C and 650°C (below eutectic) hot cylinder temperatures. The HP/TESU was preheated to approximately 500°C prior to VM start-up. The first heating half-cycle was conducted at the 1200 watt rate, followed by a one-hour discharge. The data illustrate several interesting characteristics. Note that during the first heat/cool cycle (600°C/500°C), the cold stage temperature varied significantly during the discharge of the unit. During the
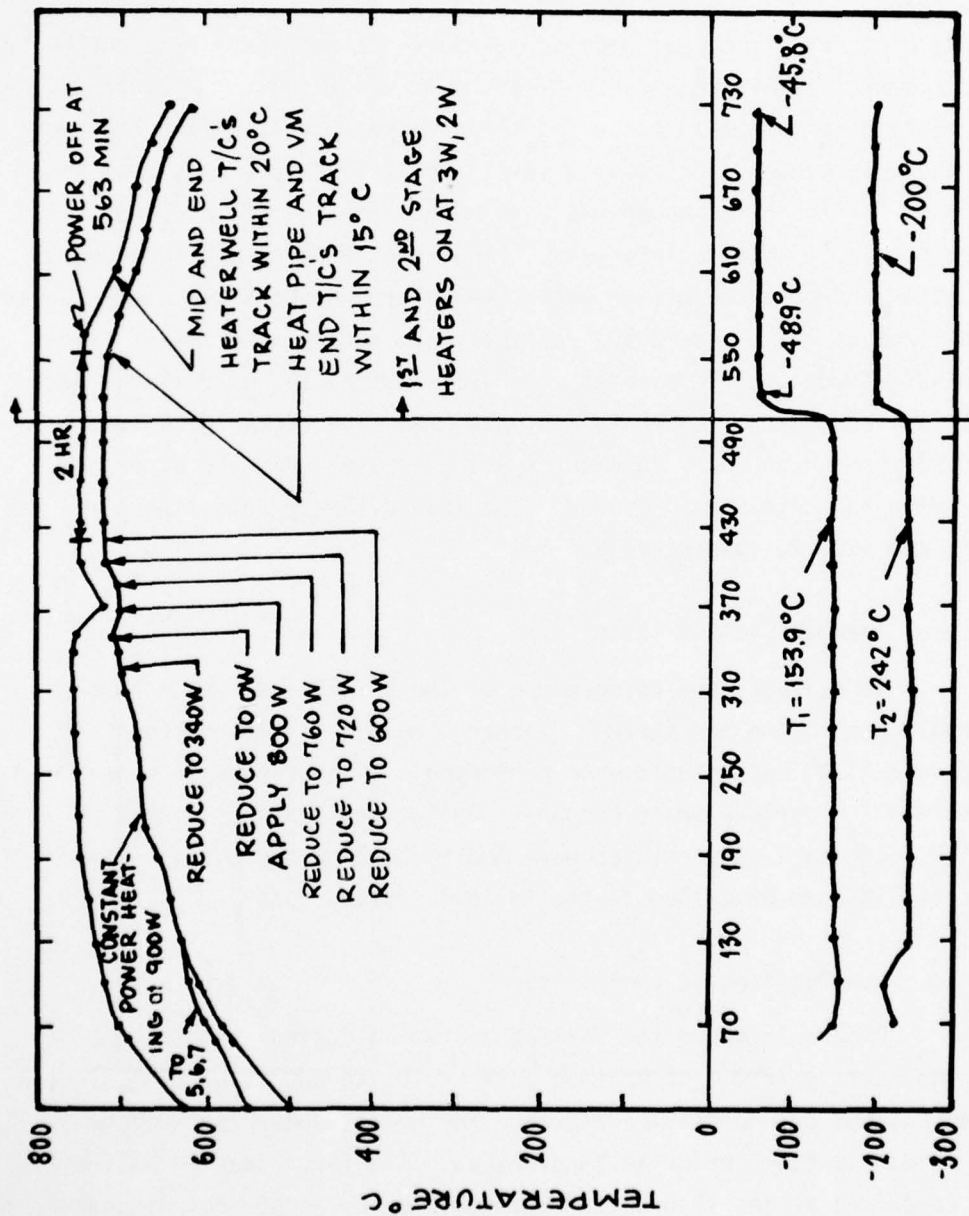
31

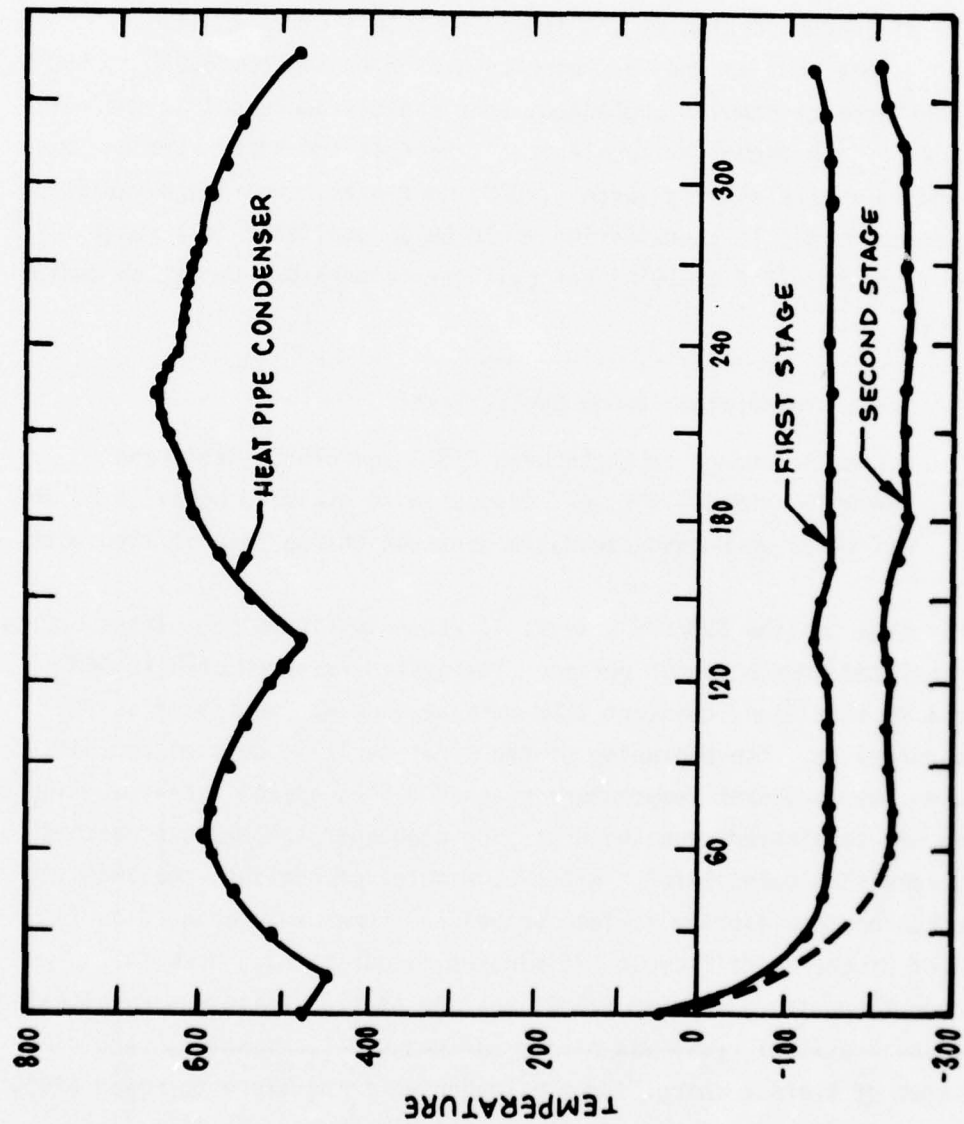Figure 14. HP/TESU-VM Start-Up Transient Performance and Dynamic Equilibrium

32

Figure 15. HP/TESU-VM Capacitive Performance at 600°C and 650°C
Maximum Hot Cylinder (Condenser) Temperature

33

second heat/cool cycle (650°C/500°C), the VM performance approaches
nominal no-load temperatures obtained during the dynamic equilibrium
testing. At the completion of the second heat half cycle (650°C cut-off),
the VM has nearly equilibrated.

The discharge portion of the second heat/cool cycle is also of
interest. Note that as the heat pipe condenser cools from 650°C to 550°C
the VM performance remains unchanged, then rapidly decreases as the rate
of cooling of the condenser accelerates. Because the VM performance was
unchanged over a relatively large (100°C) condenser temperature variation
it was decided that further testing would be accomplished in a range
greater than the ±25°F (13.9°C) hot cylinder temperature variation design
objective.

e. Design Temperature Range Cyclic Tests

Charge/discharge tests between 625°C and 675°C, 625°C and
690.6°C, and 657°C and 690.6°C were conducted to evaluate behavior of the
system. All tests were conducted at a constant charge rate of 1200 watts.

The data for the 625/675°C tests is shown in Figure 16. Three cycles
were completed over a 9-hour period. The system was preheated to 500°C
with the VM shut down; constant 1200 watt heating was initiated as the
VM was turned on. The beginning of the first cycle is defined as that
time when the condenser temperature reached 625°C, approximately 66 minutes.
Heating was terminated when the heat pipe condenser temperature reached
675°C, some 53 minutes later. After 56 minutes of heating, the VM cold
stages reached equilibrium no-load values and remained unchanged during
the first discharge half cycle (75 minutes in duration). When the
condenser temperature reached 625°C, heating at 1200 watts was reinitiated.
The second heat/cool cycle was performed in a similar fashion, requiring
65 minutes of thermal charge for the condenser temperature to reach 675°C.
At the completion of the second (68 minute) discharge, the first and
second stage loads were applied and the system was again heated at the
1200 watt rate of 675°C. At the completion of the third heat half cycle, an
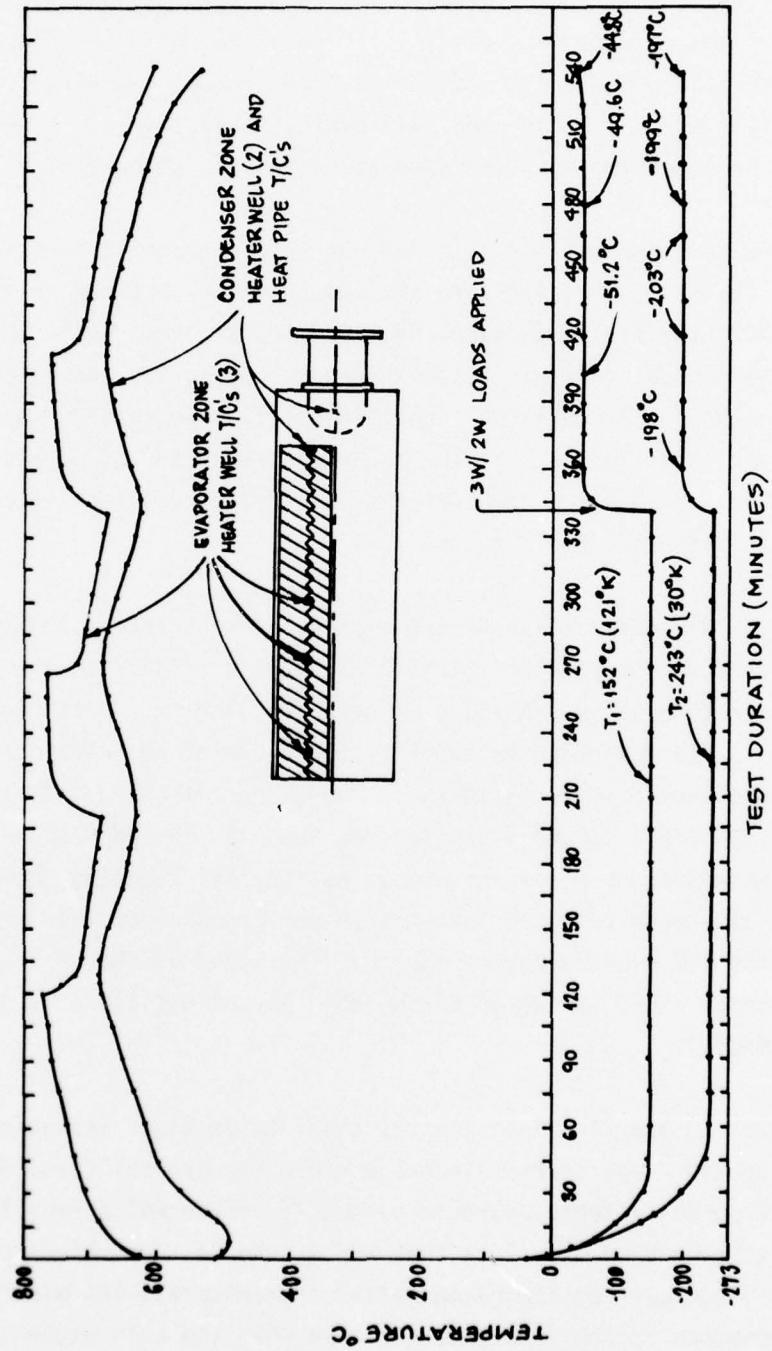extended cool-down half cycle was performed, discharging the system for

34

Figure 16. Charge/Discharge Cyclic Tests Between 625°C and 675°C

35

2 hours.   Note that, at the end of this third discharge half cycle, the
HP/TESU was remarkably close to the initial (starting) temperatures of
the first charge half cycle. Figure 17a and b reveal the time-temperature
symmetry of the results more clearly. Figure 17a shows the elapsed heating
time between 625°C and 675°C and the elapsed thermal discharge time
between 675°C and 625°C for each half cycle, respectively. Figure 17b
presents the superimposed time-temperature for the three cycles.

Figure 18 shows similar data for charge/discharge tests between
690°C and 625°C. The results are similar to those obtained in the
675°C/625°C. The first discharge required 100 minutes, while the second
required 90 minutes. It was noted, however, during the second charge
half cycle (at t = 315 minutes), that the watt meter setting was 1175
watts rather than 1200 watts. The power was reset to the correct level
at that time. Cold stage temperatures obtained were slightly lower than
obtained in the 675°C/625°C tests.

Figure 19 shows similar data for constant heat rate (1200W) charge/
discharge tests between 690°C (1275°F) and 657°C (1215°F). The cold
stage temperature scales are expanded here for clarity. Both the first
and second stage temperatures exhibit a near phaselike relationship with
the condenser temperature variation. The charge/discharge time between
657°C and 690°C are markedly similar, as observed in the 625°C tests,
with the exception of the first charge half cycle, requiring only 38
minutes. It should be noted that the VM performance remained essentially
constant for 150 minutes during the third extended discharge. The hot
cylinder temperature variation during this period was approximately 100°C
(690°C/590°C).

Figures 20 and 21 illustrate the axial temperature variation with
time during the final charge/discharge cycle between 657°C and 690°C.
The heat pipe axial temperature is virtually isothermal during the
charge/discharge process. Note that the discharge temperature profile
(Figure 21) becomes non-isothermal after approximately 145 minutes.
This corresponds approximately to the time when the cold stage temperatures
were observed to rise, as shown in the last discharge half cycle, shown in
Figure 19.

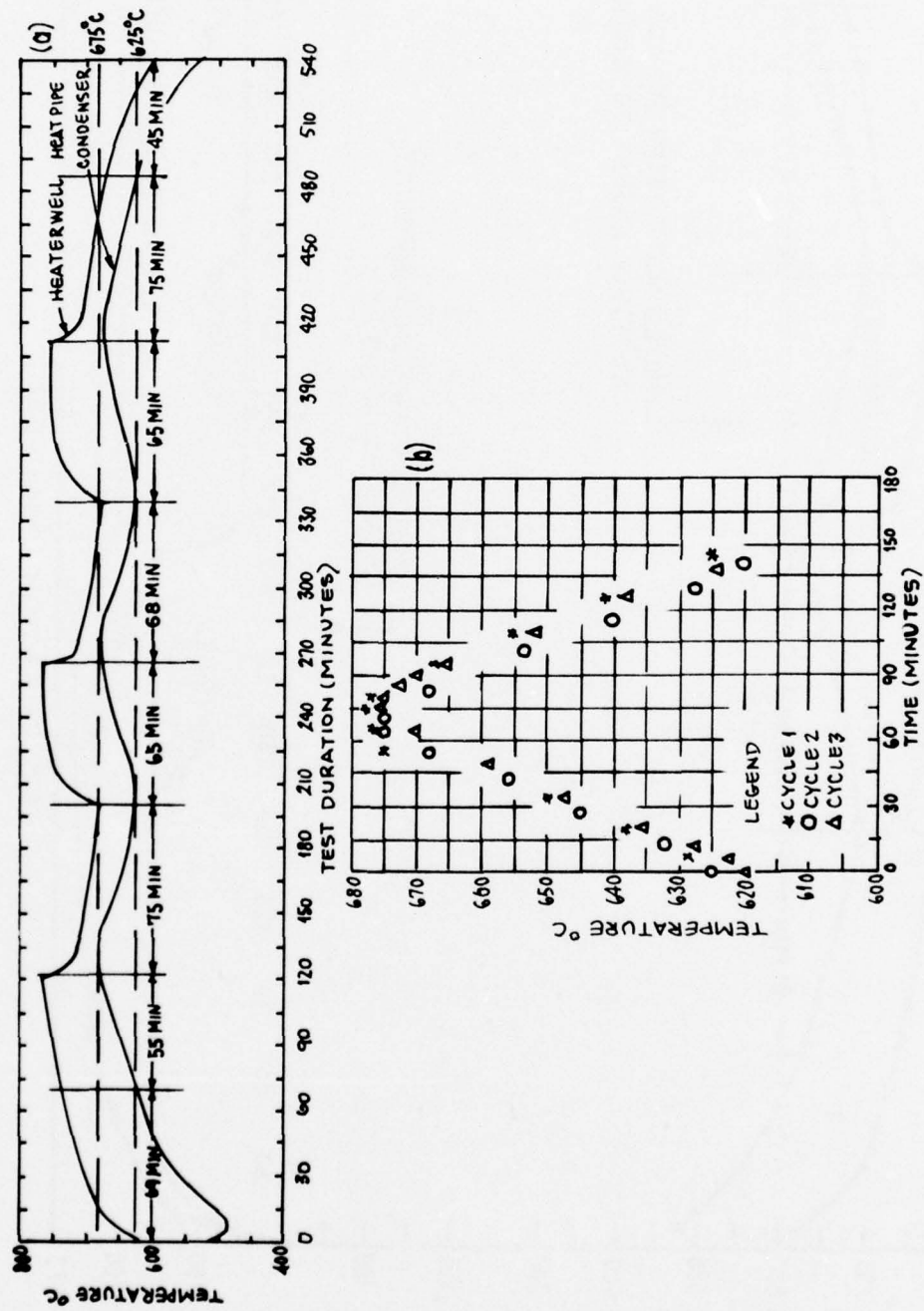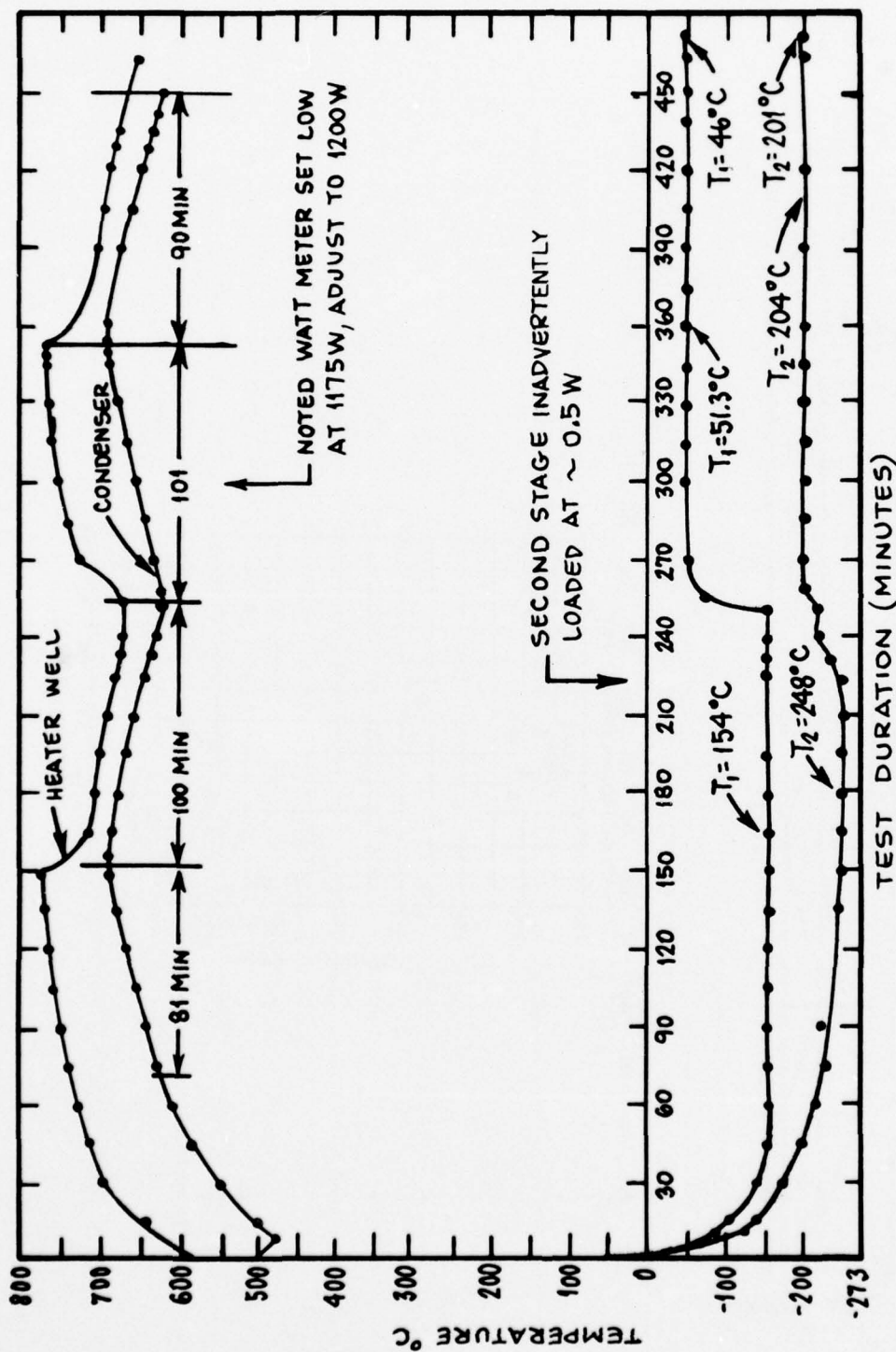Figure 17(a&b)   HP/TESU Temperature/Time Variation in 625°C/675°C Cycling

37

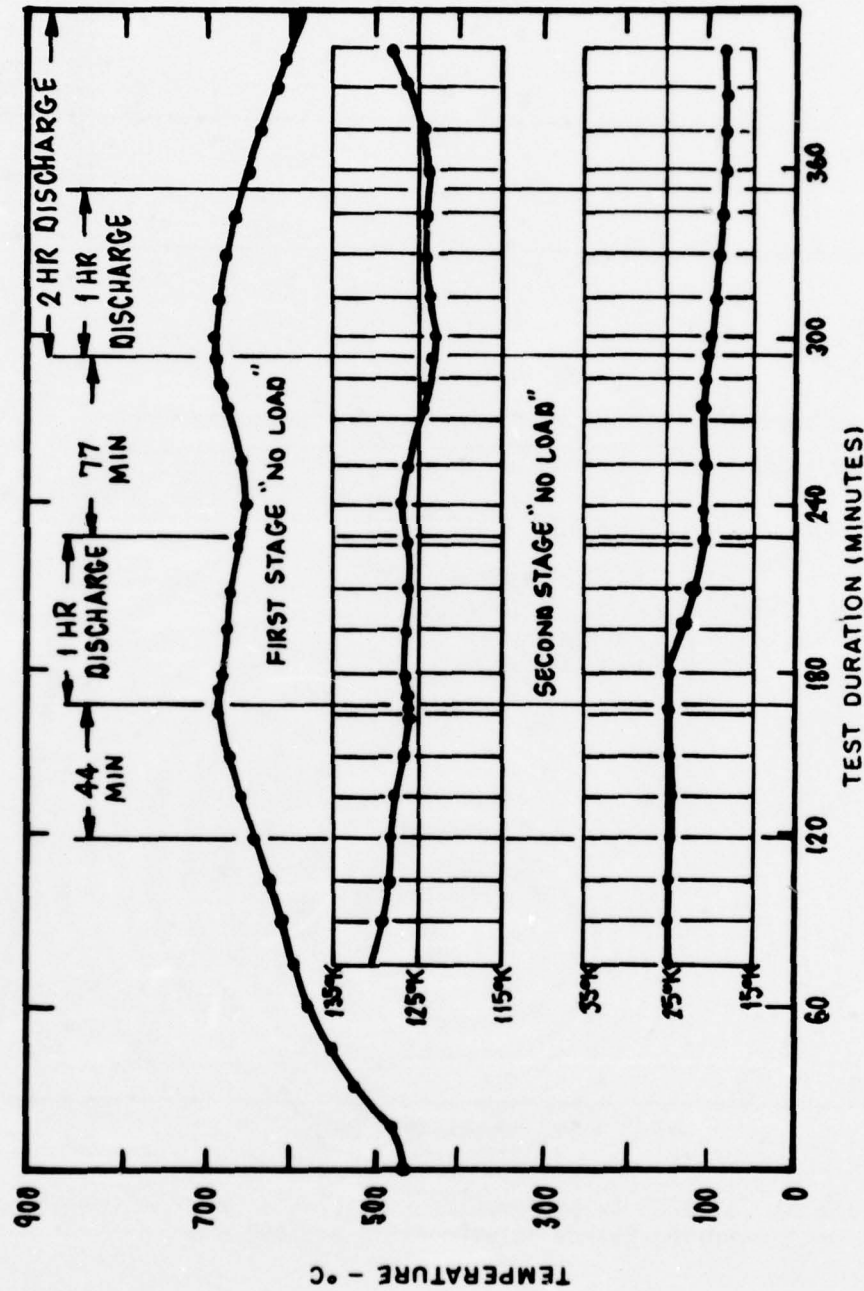Figure 18. HP/TESU-VM Cyclic Performance Between 625°C and 690.6°C

Figure 19. HP/TESU-VM Cyclic Performance Between 657°C and 690.6°C
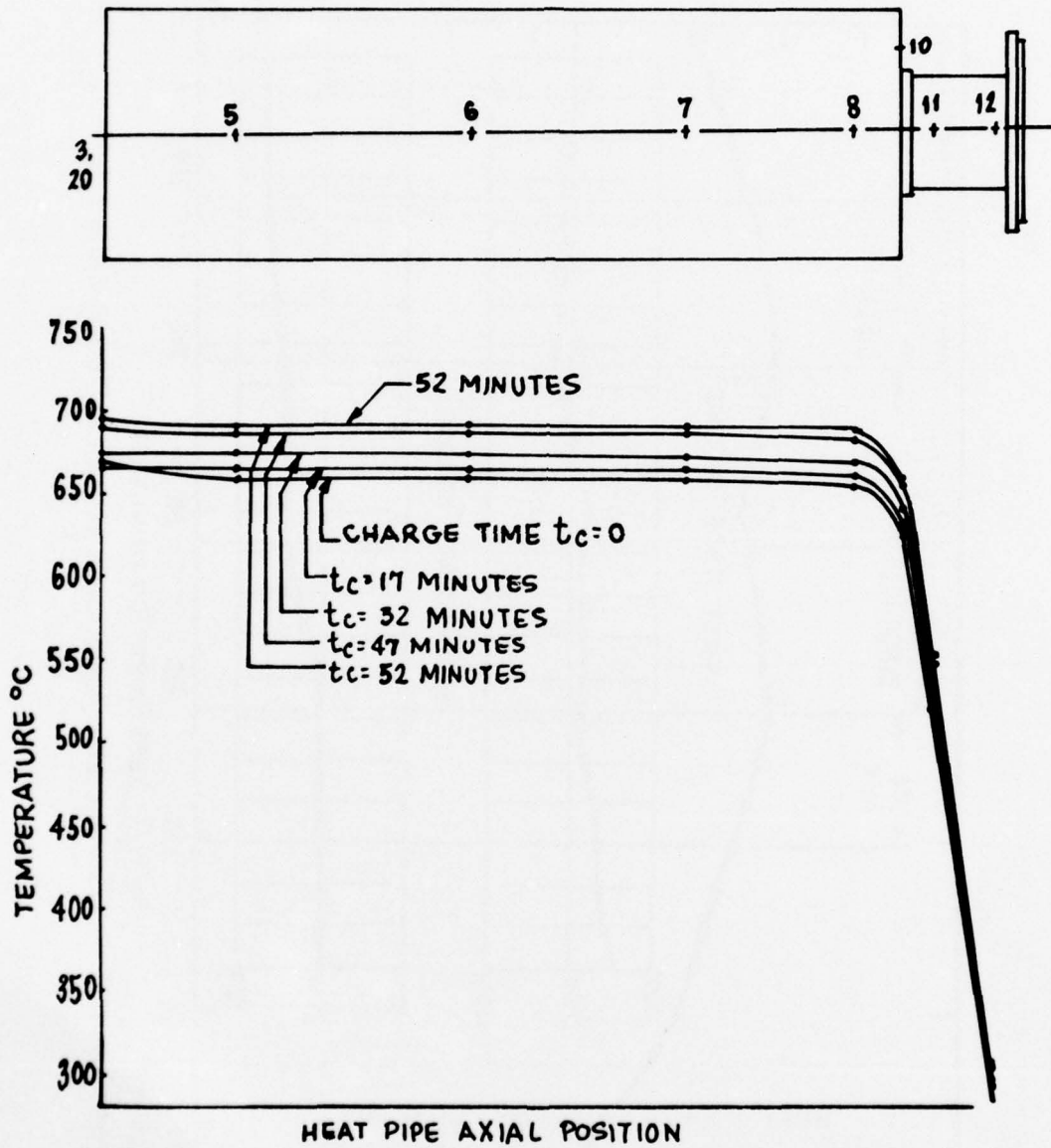
Figure 20. HP/TESU Axial Temperature Variation With VM Operating During Charge Between 657°C and 690.6°C
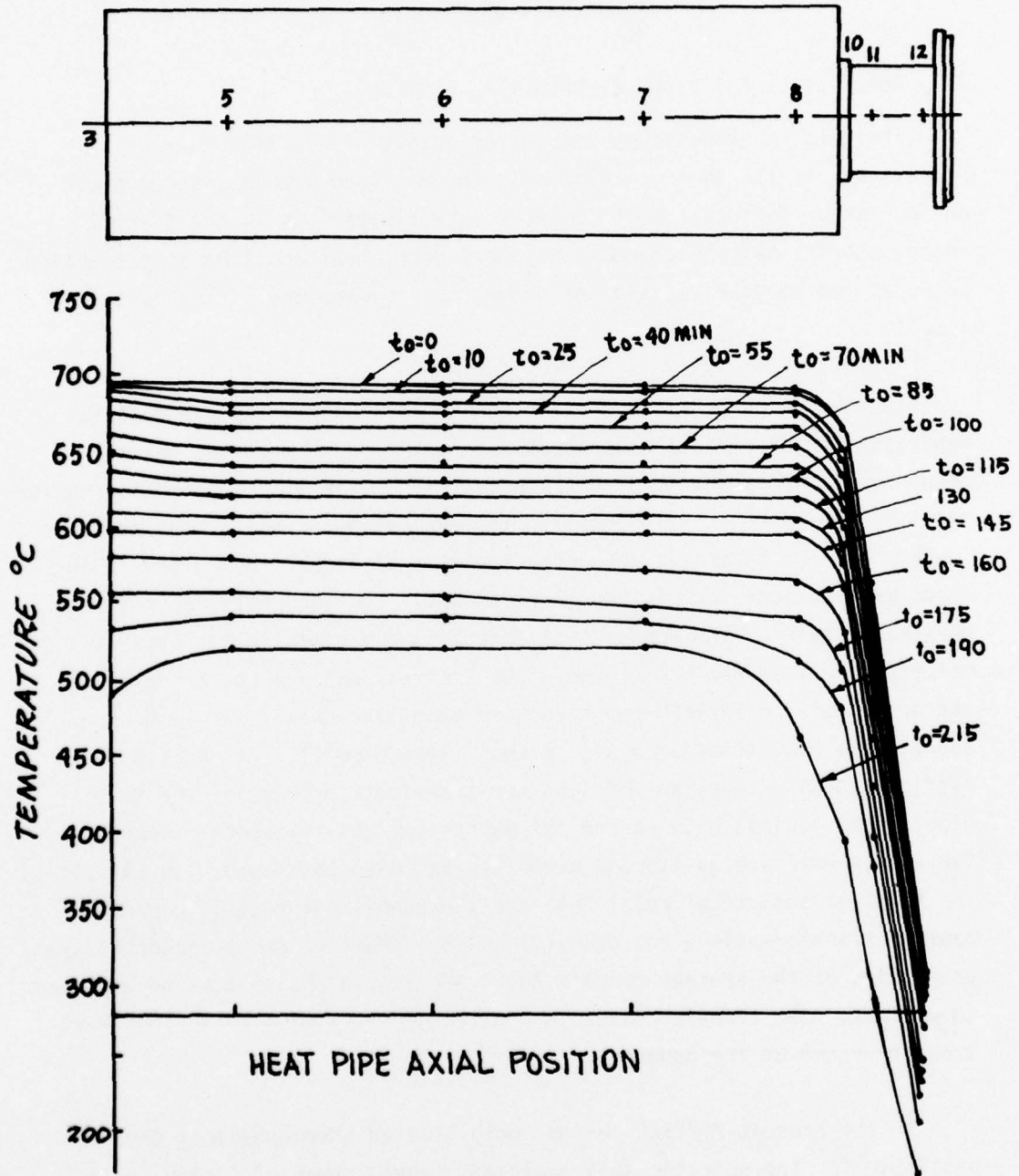
Figure 21. HP/TESU Axial Temperature Variation With VM Operating During Discharge Between 690.6°C and 520°C

SECTION IV

ANALYSIS OF RESULTS

1. ANALYTICAL DESIGN AND EXPERIMENTAL RESULTS

The rate of temperature and energy output of a HP/TESU during operation with the VM or calorimetric thermal load depends, in general, on four major factors: heat transfer rate limitations in the thermal energy storage material, and in the heat pipe, heat addition or extraction rates at the boundaries, and the geometrical dimensions of the system itself.

In the present HP/TESU design, the thermal energy storage material separates the electrical heat input and heat pipe so that the thermal response of the system is governed primarily by the transient heat transfer rates in the eutectic salt itself. The evaluation of heat transfer rates in phase change materials are among the most difficult to analyze in an exact mathematical formulation (Reference 6). Consequently, approximate physical models of the actual heat transfer mechanisms in the phase change material are frequently employed. The analysis employed by Xerox/EOS in the design of the HP/TESU represents an excellent example of such an approximate heat transfer design method (Reference 1). Xerox also faced difficult design tasks in modeling the transient response of the heat pipe. Only minimal data on the thermophysical and transport properties for the thermal energy storage materials has been cataloged. In all but the simplest analytical model both the thermophysical (specific heat, heat of transformation, and density) and transport (thermal conductivity) properties of the storage media's solid and liquid phases must be employed to evaluate heat transfer rates in a given geometry with prescribed heat transfer rates at the boundary.

In the present HP/TESU design, only limited thermophysical data was available for the eutectic salt employed, namely, heat of fusion, solid density, and transformation temperature. No data on liquid density, heat of mixing, or thermal conductivity were available. To complete the

design, assumptions concerning these properties were employed. The thermal conductivity of the selected ternary (Reference 9) $LiF-MgF_2-KF$ was taken as that of pure LiF, approximately 5.0 Btu/hr ft°F. When the HP/TESU was fabricated and tested calorimetrically, with a hot cylinder flow insert, it was found that the unit would deliver only approximately one-half the design energy storage within the specified ±25°F hot cylinder temperature variation. Xerox/Electro-Optical Systems attributed this to anomalous (non-eutectic) behavior in the salt itself, and suggested that the reported heat of fusion may be erroneous. Measurements performed by the University of Dayton Research Institute (Reference 7), using drop calorimetric methods, showed that the heat of transformation was approximately 85% of ideal as reported by Baruka (Reference 8), which was also approximately the same value (788 joules/gm) reported to Xerox/Electro-Optical Systems by North American Phillips Corporation (Reference 1). Further differential thermal analyses (DTA) examinations of the ternary eutectic revealed no other major thermal events (phase changes) in the vicinity of the melting temperature. An alternate explanation of reduced energy storage of the device was hypothesized by the Air Force Aero Propulsion Laboratory investigators concerning the salt thermal conductivity. A thermal conductivity value of approximately one-half that assumed would explain the observed discrepancy in attainable stored energy within the design ±25°F variation.

2. DETERMINATION OF EFFECTIVE THERMAL CONDUCTIVITY OF HP/TESU

Under steady state heat transfer conditions, the temperature gradients measured between the heater well and heat pipe can be employed to estimate the apparent or effective thermal conductivity of the HP/TESU. Because the inner heat pipe was not instrumented with thermocouples, it is necessary to assume that the vapor temperature in the inner and outer heat pipe are the same. With that assumption, the HP/TESU can be modeled in the steady state using a simple radial resistance heat transfer model commonly employed in the analysis of radial heat transfer through cylindrical walls (Reference 6). The effective thermal conductivity method is commonly used in characterizing heat transfer in porous or multiphase materials. The nomenclature effective (rather than actual) thermal

conductivity is employed because the salt volume and phase state are a function of temperature, as is the percentage of each phase present at temperatures just above the eutectic temperature under conditions of non-equilibrium (i.e., conduction heat transfer). Figure 22 shows the initial start-up of the heat-up under these conditions which was performed with the VM installed but not operating (motor off).

3. EFFECTIVE THERMAL CONDUCTIVITY MODEL AND EXPERIMENTAL DATA

Consider the concentric heater well thermal storage heat pipe configuration shown in Figure 23. The heat flow from the heater well to vapor space of the inner and outer heat pipe regions is in parallel, that is, the heat transfer is both radially outward and radially inward to the heat pipe zones. Let $\dot{Q}_o$ and $\dot{Q}_i$ be the steady state heat transfer rates in the outer and inner directions, respectively. The total steady heat flow is then

$$\dot{Q}_t = \dot{Q}_o + \dot{Q}_i = \frac{T_h - T_{wo}}{\frac{1}{2\pi kL} \ln \frac{r_{wo}}{r_{ho}}} + \frac{T_h - T_{wi}}{\frac{1}{2\pi kL} \ln \frac{r_{hi}}{r_{wi}}} \qquad (1)$$

The inner and outer heater wall radii, r_{hi} and r_{ho}, are known dimensions, as are the inner and outer wall radii, r_{wo} and r_{wi}, and the length L. The inner and outer wall temperatures T_{wo} and T_{wi} (bounding the inner and outer thermal energy storage material and heat pipes) are not known, but may be estimated in the following manner. Let the heat pipe vapor temperatures in the outer and inner heater well be T_{vo} and T_{vi}. Neglecting the temperature gradient in the Inconel walls and the boiling and condensing temperature gradients in the heat pipe regions, then T_{wo} and T_{wi} are equal to T_{vo} and T_{vi}, respectively. Further, the inner and outer heat pipe vapor temperatures, T_{vo} and T_{vi} are assumed equal, thus the total heat transfer rate $\dot{Q}_T$ becomes

$$\dot{Q}_T = (T_h - T_v) \frac{[\ln \frac{r_{hi}}{r_{wi}} + \ln \frac{r_{wo}}{r_{ho}}] 2\pi kL}{[(\ln \frac{r_{hi}}{r_{wi}}) (\ln \frac{r_{wo}}{r_{hi}})]} \qquad (2)$$
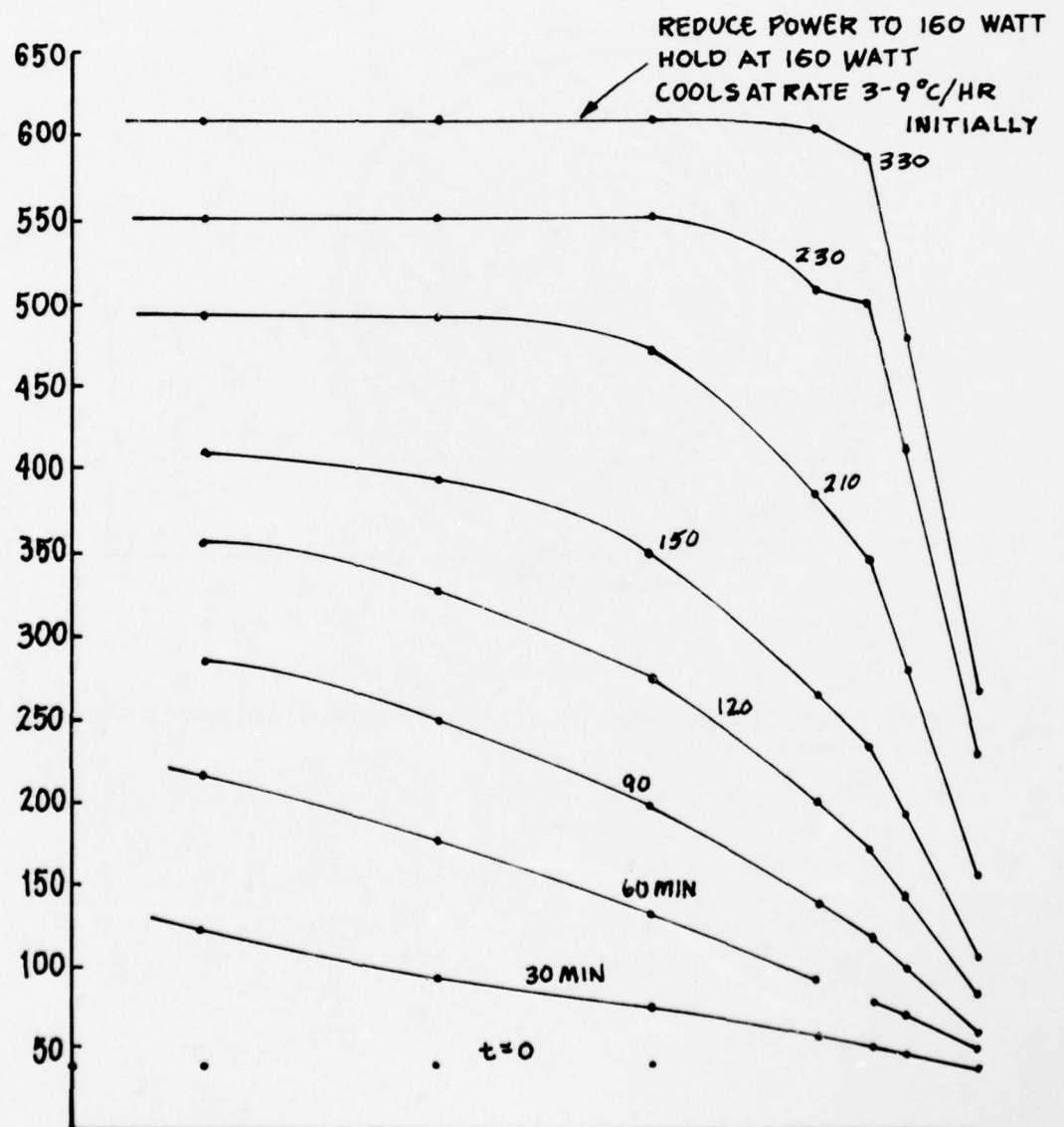
44
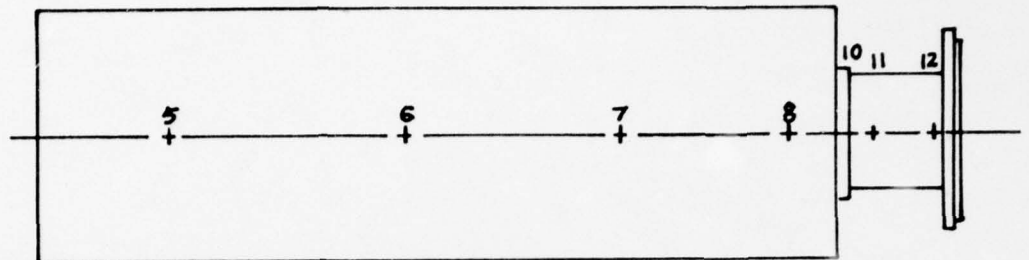
Figure 22.   HP/TESU Start-Up During Equilibrium Test With VM Off
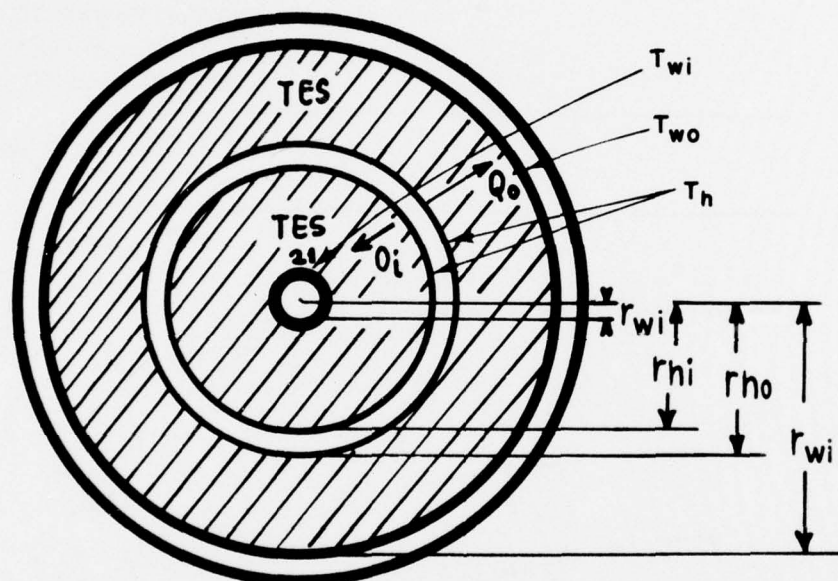
Figure 23. Geometry and Nomenclature for Effective Thermal Conductivity
Model

AFAPL-TR-77-10

Solving for k, the effective thermal conductivity, we get

$$k = \frac{\dot{Q}_t}{2\pi L} \quad \frac{1}{T_h - T_v} \quad \frac{\left[\ln \frac{r_{hi}}{r_{wi}} \times \ln \frac{r_{wo}}{r_{ho}} \right]}{\left[\ln \frac{r_{hi}}{r_{wi}} + \ln \frac{r_{wo}}{r_{ho}} \right]}$$

(3)

The apparent or effective thermal conductivity is evaluated by substituting experimental $(\dot{Q}_T, T_h, T_v)$ and geometric data into Equation 3. A sample calculation is shown below for the 240 watt radiatively cooled case.

$$k = \frac{240w}{(2\pi)(35cm)} \quad \frac{1}{647.4°C - 605.5°C} \quad \frac{\left[\ln \frac{2.7\ cm}{0.6\ cm} \times \ln \frac{5.4\ cm}{3.3\ cm} \right]}{\left[\ln \frac{2.7\ cm}{0.6\ cm} + \ln \frac{5.4\ cm}{3.3\ cm} \right]}$$

$$k = \frac{0.0096w}{cm°C} = \frac{1.79\ Btu}{ln\ ft\ °F}$$

Experimental data were taken for the system completely insulated, the hot cylinder freely radiating, and with heat transfer to the VM with the motor both on and off. The data are presented in Table III, with T_h being the average heater well temperature and T_v being the mean axial heat pipe temperature. In the design temperature range, the effective thermal conductivity is approximately 3.0 Btu/hr ft °F as shown in Figure 24. This value is 40% less than that employed in the Xerox/EOS design analysis, and it is thought that the discrepancy observed in energy output/hot cylinder temperature variation can be explained (at least in part) by this fact.

4. CHARGE/DISCHARGE ENERGY BALANCE CALCULATIONS

The thermal cycling data presented in Figure 15 (675°C/625°C), Figure 16 (690.6°C/625°C), and Figure 18 (690.6°C/657°C) can be evaluated as follows. Consider the HP/TESU as a control volume and neglect all rate-limiting energy transfer mechanisms (e.g., capacitive heating, phase change, conduction, convection, and radiation). From the first law of thermodynamics

$$E_{in} = E_{out} + E\ stored$$

(4)

47

TABLE III

EFFECTIVE THERMAL CONDUCTIVITY DATA

Test	Applied Power	T_H	T_V	$\Delta T = T_H - T_V$	k Btu/hr ft °F
Fully Insulated	50W	230°C	215.4°C	14.6°C	1.08
	100W	468.7°C	446.9°C	21.8°C	1.45
	150W	621.6°C	600.4°C	21.2°C	2.21
	200W	708.4	688.4°C	15.0°C	4.20
Radiatively Cooled Hot Cylinder	240W	647.5°C	605.5°C	42°C	1.80
	300W	710.1°C	693.7°C	16.4°C	5.76
	340W	740.7°C	724.9°C	10.1°C	10.56
VM Operating	600W	674.4°C	600.4°C	74°C	2.55
	600W	737°C	715.6°C	21.4°C	8.83
	800W	776.4°C	599.2°C	177.2°C	1.42
	1000W	712.2°C	593.3°C	119.6°C	2.63
	1000W	819.9°C	790.4°C	29.5°C	10.66
	1000W	774°C	743.1°C	30.0	10.49
	1000W	741.1	702.9	38.2	8.255
VM Installed, Motor Off					
	160W	554.1°C	523.3°C	30.8°C	1.636
	180W	560.0°C	527.7°C	32.3°C	1.75
	200W	582.7°C	550.75	31.95°C	1.97
	250W	681.5	653.36	28.14°C	2.79
	264W	710.45	680.95	29.5	2.81
	308W	718.7	689.9	28.76	3.37
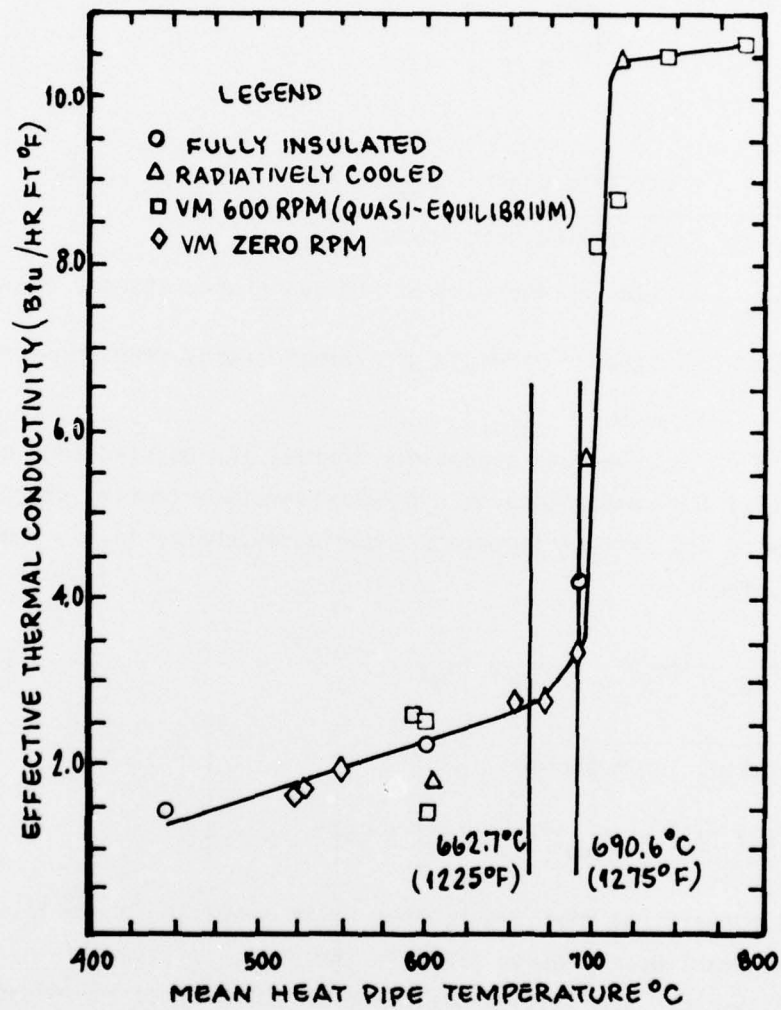
Figure 24. Effective Thermal Conductivity vs Temperature

Writing Equation 4 in terms of the charge and discharge rates, assuming the power consumption of the VM, P_{vm}, and insulation losses, $\dot{Q}_1$ are constant over a cycle, results in the following

$$E_{in} = P_c \cdot t_c = P_{vm} (tc + td) + \dot{Q}_e (tc + td) + \dot{Q}_{TES_c} \cdot t_c \qquad (5)$$
$$- \dot{Q}_{TES_d} \cdot t_d$$

where

P_c = electric power input to HP/TESU during charge

$\dot{Q}_1$ = insulation heat losses

$\dot{Q}_{TES_c}$ = rates of increase of thermal energy storage during charge

$\dot{Q}_{TES_d}$ = rates of decrease of thermal energy storage during discharge

If the HP/TESU undergoes a complete thermal charge/discharge cycle, from an initial low temperature to a high temperature (during charge) and then returns to its initial temperature during discharge (i.e., thermodynamic state), then

$$(\dot{Q}_{TES_c}) (t_c) = (\dot{Q}_{TES_d}) (t_d) \qquad (6)$$

so that Equation 5 becomes

$$(P_c) (t_c) = (P_{vm}) (t_c + t_d) + (\dot{Q}_1) (t_c + t_d) \qquad (7)$$

Consider the first discharge/charge cycle shown in Figure 15, neglecting initial start-up charge to 675°C in the analysis of cyclic performance of the system. The initial discharge to 625°C requires 75 minutes, with subsequent charge back to 675°C at a constant charge rate of 1200 watts requiring 65 minutes.

Solving Equation 7 for P_{vm}, we obtain

$$P_{vm} = \frac{P_c \cdot t_c - \dot{Q}_1 (t_c + t_d)}{t_c + t_d} = P_c \left(\frac{t_c}{t_c + t_b} - \dot{Q}_1\right) \qquad (8)$$

By substituting t_d = 1.25 hr, t_c = 1.0833 hr, P_c = 1200 watts, and $\dot{Q}_1$ = 200 watts into Equation 8, we find P_{vm} to be

$$P_{vm} = 1200W \left(\frac{1.0833}{2.333}\right) - 200W = 357.2 \text{ watts}$$

The surprisingly low VM power consumption is difficult to explain based on the nominal input power rates documented in References 2 and 3, although Hughes reported power consumptions as low as 300 watts for "off-design" operation. Figure 25, extracted from Reference 2, shows predicted heater power requirements for fixed, elevated (100°K) first stage temperatures, with second stage temperature as the independent variable. These analytical data validate the apparent low power assumption values calculated using Equation IV-8.

Table IV summarized the energy balances for all fixed charge/discharge temperature tests described in Section III and several additional single cycle tests not reported in Section III, assuming $\dot{Q}_1$ = 200 watts. The calculated VM power consumption ranges from 345W to 404W for cyclic tests, approximately a 15% variation. Because these values were so low, it was decided to test the VM in the electrically heated configuration again, measuring the actual power consumption of the heaters.

A direct correlation of VM performance with the electrically heated hot cylinder is difficult for several reasons. First, VM performance was found to vary slightly from test to test for both configurations (due in part to pressure losses, purge condition). Secondly, a pronounced hot cylinder capacitance effect appears when the "cool down" curve of the electrically heated VM is compared to the extended discharge curves for the HP/TESU-VM configuration. Note that in Figure 7 the rapid rate of change of the first and second stage temperatures (approximately 40-50°C) as the hot cylinder temperature decreases from 690°C to 600°C. Cold stage temperature variations during 100°C cooling in the HP/TESU configuration are approximately one order of magnitude less, as shown in Figure 16, 18, and 19. This capacitive effect points out that requirement for temperature regulation within ±25°F may be overly restrictive unless cold stage temperatures must be maintained without small variance (±2°C).
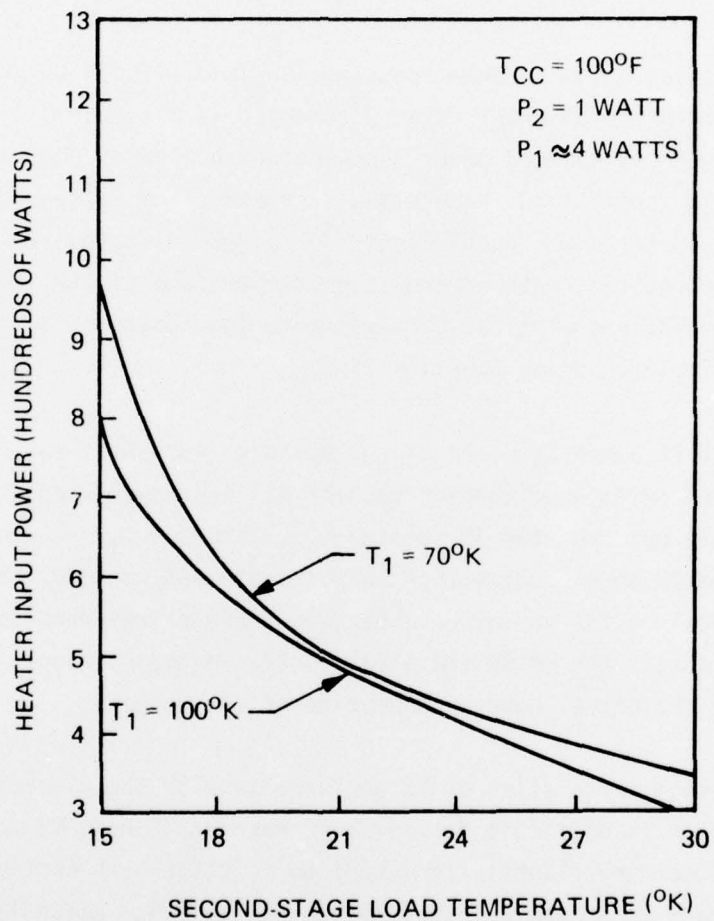
Figure 25. VM Heater Power (at $T_1 = 100°K$) as a Function of T_2

TABLE IV

ENERGY BALANCE CALCULATIONS FOR CYCLIC TESTS

Test	Cycle No.	Discharge Time	Charge Time	Pvm (as calcul. from Eq. 8)	T_1T_2	VM Load
675/625°C	1 of 2	75 min	65 min	357.2W	-152, -243°C	o/ow
675/625°C	2 of 2	68 min	65 min	385.56W	-51, -203°C	3/2w
690.6/625°C	1 of 1	101 min	100 min	397.1W	-51, -203°C	3/2w
690.6/657°C	1 of 2	60 min	50 min	345.4W	-147, -242°C	ow/ow
690.6/658°C	2 of 2	61 min	52 min	352.2W	-143, -242	ow/ow
650/610°C	1 of 1	50 min	43 min	354W	-153, -245	ow/ow
690.6/650	1 of 1	66 min	67 min	404.5W	-152, -255°C	Best ow/ow

The second electrically heated hot cylinder test sequence yielded interesting comparative results. The performance of the cold stages was nearly identical to that measured in the initial test sequence, -150°C, -250°C under no-load, and -51, -200°C under 3W, 2W load conditions. The total heater powers for these respective load conditions were 500 watts and 600 watts, respectively, with the hot cylinder and crankcase temperatures of 670°C and 49°C, respectively, with motor speed measured at 500-600 rpm. Hence it is concluded, that within the inherent experimental error and calculation procedures outlined above, the power consumption of the VM is reduced by approximately 30% while being heated by the HP/TESU.

5. HP/TESU AND ELECTRICALLY HEATED VM PERFORMANCE ASSESSMENT

Table V summarizes the HP/TESU-VM test results in a manner similar to the electrically heated VM test results presented in Table II. Data in Table V includes both cyclic test results (at the beginning and end of charge), start-up (quasi-equilibrium) and equilibrium test results. The crankcase temperature for all data reported is in the range of 44 to 48°C.

The cyclic results cited in Table IV illustrate the cold stage temperature variation during cycling. The largest variation appears consistently in first stage, with a maximum change of 3°C. Larger variations for extended discharges, beyond the energy storage design goal of the HP/TESU, are also shown.

The steady-state and start-up data reported illustrate that condenser/hot cylinder temperature has very little influence on cold stage performance; the 800°C, 3W/2W data is nearly identical to the steady-state 718°C data and cyclic data for the same loads. It is concluded that the heat transfer is limited by the VM, not the HP/TESU.

In comparison with the electrically heated VM test results (Table II) no clear cold stage advantage for either configuration is evident for tests where the crankcase temperatures were similar, although the power consumption reduction of the VM with the HP/TESU clearly illustrates the enhanced effectiveness of the unit.

TABLE V

HP/TESU-VM TEST RESULTS SUMMARY

Test	Condenser (Hot Cylinder) Temperature	1st Stage Temperature	2nd Stage Temperature	
Cycle 1 of 3	675°C	-152.2°C	-244°C	ow/ow, 75 min discharge
	625°C	-152.2°C	-244°C	
Cycle 2 of 3	675°C	-153.1°C	-243°C	ow/ow, 75 min discharge
	620°C	-152.2°C	-242°C	
Cycle 3 of 3	675°C	-51°C	-199°C	3w/2w, 68 min discharge
	625°C	-49.6°C	-199°C	
	528.6°C	-44.8°C	-197°C	3w/2w, 2.33 hr discharge
Cycle 1 of 2	690.6°C	-155°C	-246°C	ow/ow, 100 min discharge
	625°C	-154.5°C	-247°C	
Cycle 2 of 2	690.6°C	-51.3°C	-203°C	3w/2w, 90 min discharge
	625°C	-47.6°C	-201°C	
	600°C	-46°C	-201°C	3w/2w 2.0 hr discharge
Cycle 1 of 2	690.6°C	-148.7°C	-240°C	ow/ow, 60 min discharge
	658°C	-145.7°C	-242°C	
Cycle 2 of 2	690.6°C	-146.4°C	-242°C	ow/ow, 60 min discharge
	658°C	-147.4°C	-240°C	
Cycle 3 of 3	690.6°C	-145.8°C	-243°C	ow/ow, 60 min discharge
	658.0°C	-144.0°C	-243°C	
	617.7°C	-145.0°C	-243°C	ow/ow, 2 hr discharge
	520.0°C	-140.6°C	-240°C	ow,ow, 3 hr discharge
Cycle 1 of 2	690.6°C	-147°C	-249°C	ow/ow, 1 hr discharge
	650°C	-146.9°C	-251°C	
Cycle 2 of 2	690.7°C	-150.3°C	-253°C	ow/ow, 66 min discharge
	646.0°C	-149.3°C	-255°C	
	601.1°C	-145.4°C	-255°C	ow/ow, 2 hr discharge
Start-up	750°C	-158°C	-249°C	ow/ow, 4.75 hr, 1200W, 25°C
"	800°C	-55.6°C	-199.4°C	3w/2w, 5.5 hr, ~1000W
"	600°C	-154°C	-222°C	ow/ow, 1 hr, 1200W, 500°C
"	600°C	-152.6°C	-242°C	ow/ow, 8 hr, 600W, 500°C
Steady	720°C	-152.6°C	-242°C	ow/ow, 9.5 hr ~600W, 500°C
"	718°C	-48.9°C	-198°C	

The extended discharge HP/TESU-VM performance is thought to be significant and clearly shows that condenser (hot cylinder) temperature is not a good performance predictor for cold stage temperature since VM performance is essentially unchanged with relatively large ΔT's of the condensers.

The comparative performance aspects of the testing described here are not conclusive, in any sense, but are representative of the dynamic behavior of the integrated subsystems. Follow-on testing is required with improved VM diagnostic apparatus before assessment of the "on-design" dynamic behavior can be obtained.

SECTION V

CONCLUSIONS AND RECOMMENDATIONS

1. HP/TESU-VM THERMOMECHANICAL COMPATIBILITY

The integration of the VM and HP/TESU was relatively straightforward. No thermomechanical interference or compatibility problems were incurred other than the minor flange and O-ring seal problem incurred during the initial mating of the devices. Simultaneous start-up of the VM and heating of the HP/TESU was possible from both room temperature and elevated (500°C) temperature with no evidence of motor stall or high (>60°C) temperature excursion of the cold stage during the cool-down.

2. COMPARATIVE PERFORMANCE

The VM cold stage performance with the HP/TESU was essentially the same as measured with the electrically heated hot cylinder. First stage temperatures under load and no-load conditions were significantly higher (70°K) than those reported by Hughes at similar speeds, fill pressures, and hot cylinder temperatures, irrespective of the heating mode.

The input power to the VM for the elevated first stage temperatures achieved was significantly lower than the no-load (600W) and 3W/2W load (730W) conditions reported by Hughes. Further, the average net power input to the VM was significantly less with the HP/TESU due to the improved heat transfer afforded by the heat-piped hot cylinder arrangement.

3. HP/TESU CAPACITY AND PERFORMANCE

Start-up and cyclic operation of the HP/TESU-VM presented no difficulties; precise equilibrium operation (zero rate of change of temperature) was difficult to obtain. Cyclic operation of the HP/TESU with the VM between the temperature limits selected (690.6-657°C, 690.6-625°C, 675-625°C) revealed only minor first stage temperature (3°C) variation during cycling, with second stage temperatures essentially constant.

Based on the extended discharge (2-3 hour) tests, with the reduced
VM power consumption, the capacity of the HP/TESU is approximately
1.0 kw-hr within a hot cylinder temperature variation of 100°C. The
specification limiting HP/TESU hot cylinder temperature variation to
±25°F appears overly restrictive based on the observed first and second
stage temperature stability during hot cylinder temperature variations
of 100°C (see Figure 19). Similar cold stage stability was not observed
for the electrically heated configuration during hot cylinder temperature
excursions of 100°C (see Figure 7).

The stability of the VM cold stage performance during 100°C excursion
of the HP/TESU is attributed to the near constant power delivery of the
heat pipe to the hot cylinder during that excursion. Because the heat
transfer coefficient on the sodium vapor side is much higher than that on
the helium-regenerator side of the hot cylinder, the VM itself limits heat
transfer to the hot cylinder. On the other hand, the heat transfer rate
into the heat pipe is limited by the conductive resistance of the salt,
which increases as the salt layer thickness grows. When the conductive
resistance of the salt layer (neglecting its capacitance) exceeds the
convective resistance at the regenerator interface, the temperature of
the hot cylinder begins to decrease. These experimental results indicate
that the VM operates stably (as viewed from the cold stage) within large
temperature variations of the HP/TESU primarily because of the heat
transfer rate limitations on the regenerator side of the hot cylinder.

4. OTHER OBSERVATIONS

Precise calorimetric testing of the integrated HP/TESU-VM is inherently
difficult because the instantaneous heat losses and VM power consumption
cannot be measured directly during cyclic testing. The method of calculating
VM average power consumption during cycling, shown in Section IV-1, is
fairly accurate if the insulation losses are well characterized. In daily
testing of the HP/TESU-VM, start-up was accelerated by preheating the
HP/TESU to 500°C before starting the VM (motor and heat exchanger).
Similarly, because of the long cool-down period, the VM (motor and heat
exchanger) was stopped while the HP/TESU was still at elevated temperature

58

(500-600°C) with no apparent adverse effects on the VM. In essence, with the VM motor and heat exchanger turned off, the hot displacer and cold stages are thermally isolated from the HP/TESU. It is thought that the inherently long thermal equilibrium time characteristic of the HP/TESU and the thermal isolation property observed act as inherent safety features against overheating the hot cylinder.

5.   SUMMARY OF RESULTS

Operation of the VM with the HP/TESU was successfully demonstrated. By virtue of improved heat transfer to the VM hot cylinder by the heat pipe action of the HP/TESU, the net thermal power consumption of the VM was reduced by approximately 25%. The success of these results is partially offset by the fact that the VM was operating in an "off-design" condition (high first stage temperature). Should further tests prove this heat transfer advantage also exists at design conditions for the "AFLIR" and other cryocoolers, both a significant system weight saving and array sizing advantage would be offered by the HP/TESU concept.

6.   RECOMMENDATIONS

Testing of the HP/TESU with the VM should continue to further characterize the dynamic behavior of the integrated system. AFAPL has requested that AFFDL assess the technical feasibility of reworking the cooler so that "on-design" performance can be achieved.

Testing of similar HP/TESU with more advanced cryocoolers should be pursued based on the inherent energy storage density and heat transfer advantages of the concept.

REFERENCES

1. Richter, Robert, "ONE KW-HR THERMAL ENERGY STORAGE DEMONSTRATION FOR VUILLEUMIER CRYOGENIC COOLER," Xerox Electro-Optical Systems, Interim Report prepared under Contract F33615-75-C-2045, AFAPL-TR-76-110, January 1976.

2. Doody, R. D., "TWO-STAGE VUILLEUMIER CYCLE CRYOGENIC REFRIGERATION SYSTEM FOR ADVANCED FORWARD LOOKING INFRARED (AFLIR) APPLICATIONS," Hughes Aircraft Company, Final Report prepared under Contract F33615-69-C-1459, AFFDL-TR-71-17, August 1971.

3. Block, R. F., "THE DESIGN, DEVELOPMENT, AND TEST OF A HEAT PIPE INTERFACE FOR THE HOT CYLINDER OF A VM REFRIGERATOR," Paper presented at Cryogenic Cooler Conference, USAF Academy, Colorado, AFFDL-TR-73-149, Vol. I, December 1971.

4. Schröder, J., "THERMAL ENERGY STORAGE CONTROL," ASME Paper 74-WA/ Oct-1, Winter Annual Meeting, November 1974.

5. Private Communication with William Haskin and Ronald White, AFFDL/FEE, December 1976.

6. Krieth, Frank, "INTRODUCTION TO HEAT TRANSFER," International Textbook Company, Scranton, Pa., 1968.

7. Davison, Joseph E., "EVALUATION OF INORGANIC OXIDES FOR THERMAL ENERGY STORAGE," Bi-Monthly Progress Report prepared under Contract F33615-76-C-2096, 15 August 1976 (to be published as AFAPL TR).

8. Baruka, Alina, "SURVEY AND SELECTION OF INORGANIC SALTS FOR APPLICATION TO THERMAL ENERGY STORAGE," ERDA Report ERDA-59/UC-2, June 1975.

9. Richter, Robert, "SOLAR COLLECTOR THERMAL POWER SYSTEM," Xerox Electro-Optical Systems, Final Report prepared under Contract F33615-72-C-1092, November 1974.